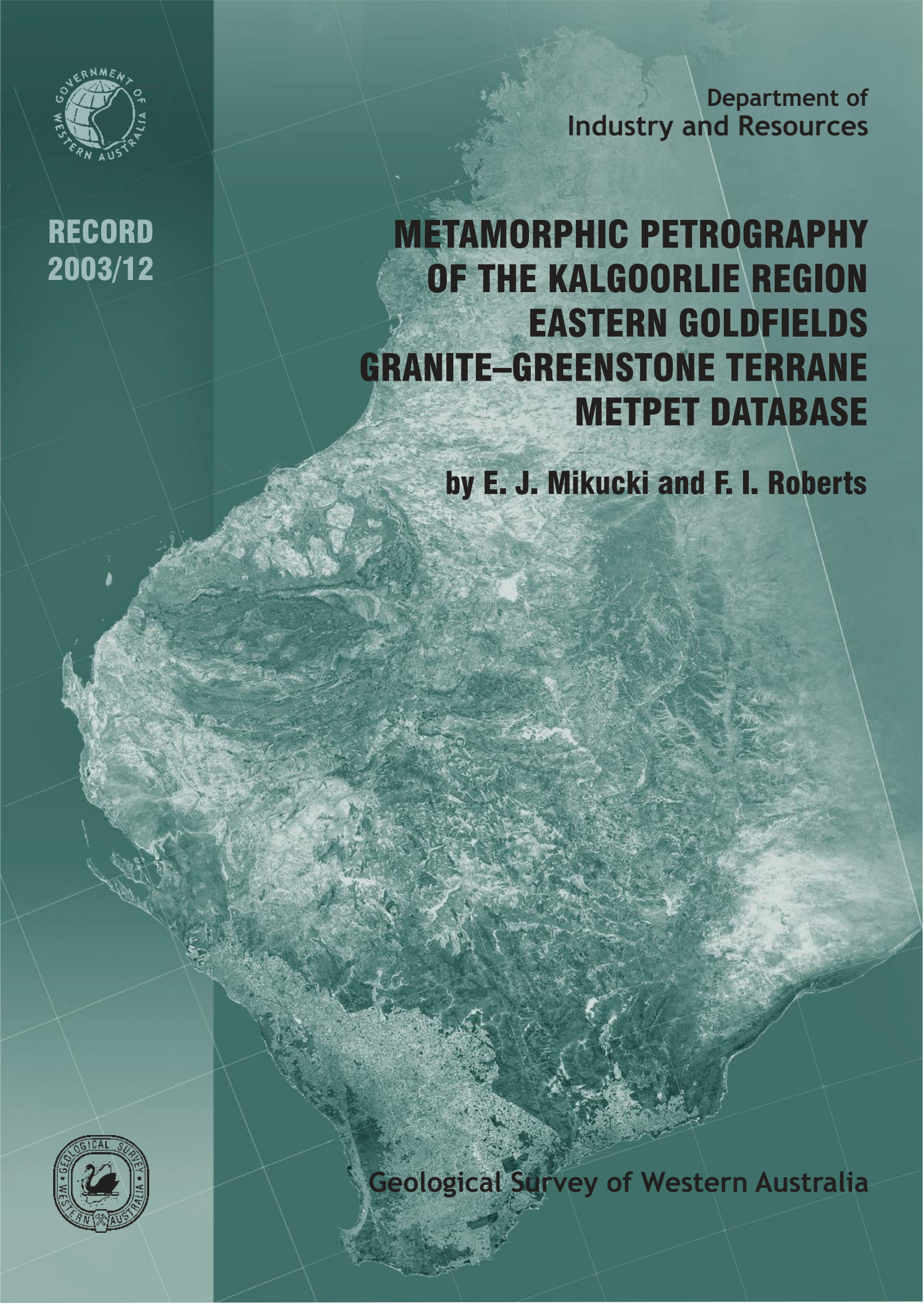

Department of
Industry and Resources

RECORD
2003/12

METAMORPHIC PETROGRAPHY OF THE KALGOORLIE REGION EASTERN GOLDFIELDS GRANITE–GREENSTONE TERRANE METPET DATABASE

by E. J. Mikucki and F. I. Roberts

Geological Survey of Western Australia

GEOLOGICAL SURVEY OF WESTERN AUSTRALIA

Record 2003/12

METAMORPHIC PETROGRAPHY OF THE KALGOORLIE REGION, EASTERN GOLDFIELDS GRANITE–GREENSTONE TERRANE: METPET DATABASE

by
E. J. Mikucki[1] and F. I. Roberts

[1] E. & J. Mikucki Geological Consultants, 2285 Coolgardie Street, Mundaring, W.A. 6073

Perth 2004

MINISTER FOR STATE DEVELOPMENT
Hon. Clive Brown MLA

DIRECTOR GENERAL, DEPARTMENT OF INDUSTRY AND RESOURCES
Jim Limerick

DIRECTOR, GEOLOGICAL SURVEY OF WESTERN AUSTRALIA
Tim Griffin

REFERENCE
The recommended reference for this publication is:
MIKUCKI, E. J., and ROBERTS, F. I., 2004, Metamorphic petrography of the Kalgoorlie region, Eastern Goldfields Granite–Greenstone Terrane: METPET database: Western Australia Geological Survey, Record 2003/12, 40p.

National Library of Australia Card Number and ISBN 0 7307 8920 9

Grid references in this publication refer to the Geocentric Datum of Australia 1994 (GDA94). Locations mentioned in the text are referenced using Map Grid Australia (MGA) coordinates, Zone 51. All locations are quoted to at least the nearest 100 m.

Published 2004 by Geological Survey of Western Australia
Cover image modified from Landsat data, courtesy of ACRES

Copies available from:
Information Centre
Department of Industry and Resources
100 Plain Street
EAST PERTH, WESTERN AUSTRALIA 6004
Telephone: (08) 9222 3459 Facsimile: (08) 9222 3444
This and other publications of the Geological Survey of Western Australia may be viewed online at www.doir.wa.gov.au/gswa or purchased online through the Department's bookshop at www.doir.wa.gov.au

Contents

Abstract 1
Introduction 1
Location 2
Geology and mineralization 2
Sample coverage 7
METPET database 8
Primary observational data 9
Interpretive data 9
Protolith groups 10
Treatment of metamorphic facies and zones 10
Metamorphic zone codes 11
Metamorphic facies 14
Pelites and semipelites 14
Quartzofeldspathic rocks 14
High-alumina rocks 16
Ultramafic rocks 16
Mafic rocks 18
Metamorphic patterns 20
Timing of metamorphism with respect to deformation 24
Relationship to granitoid plutonism 25
Hydrothermal-alteration patterns 25
Conclusion 27
Acknowledgements 28
References 29

Appendices

1. Description of digital datasets 32
2. Wallrock-alteration mineral assemblages for gold deposits in the Kalgoorlie region 33

Figures

1. Locality map of the study area in the Kalgoorlie region 3
2. Granitoid intrusions and major structures in the Kalgoorlie region 4
3. Major tectono-stratigraphic domains of the Kalgoorlie region 5
4. Precambrian geology of the Kalgoorlie region 6
5. Time–event summary of the geological history of the Kalgoorlie region 7
6. Locality map for thin-section samples 8
7. P–T diagram showing Al_2SiO_5 phase boundaries and the boundaries of the principal metamorphic facies types 11
8. Petrogenetic grid for pelitic rock types (muscovite+quartz+H_2O in excess) 15
9. Petrogenetic grid for ultramafic rock types in the CO_2-free system 16
10. Petrogenetic grid for ultramafic rock types coexisting with CO_2–H_2O fluids at 3 kbar pressure 17
11. Metamorphic assemblage map for mafic rocks 19
12. Distribution of diopside in metamorphosed mafic rocks 20
13. Metamorphic assemblage map for quartzofeldspathic rock types and pelites 21
14. Location of key pelitic and high-alumina assemblages 22
15. Distribution of metamorphic facies in the Kalgoorlie region 23
16. Distribution of hydrothermal-alteration types in mineralized mafic rocks in the Kalgoorlie region 26

Tables

1. Data fields in the METPET database 9
2. Qualitative strain index used in the METPET database 10
3. Protolith group codes 10
4. Metamorphic zone codes for major bulk rock composition groupings 12
5. Hydrothermal assemblage codes for major bulk rock composition groupings 13
6. Mineral abbreviations 14

Metamorphic petrography of the Kalgoorlie region, Eastern Goldfields Granite–Greenstone Terrane: METPET database

by

E. J. Mikucki[1] and F. I. Roberts

Abstract

Petrographic descriptions, metamorphic mineral assemblages, and spatial data for about 2000 rocks from the Kalgoorlie region of the Eastern Goldfields Granite–Greenstone Terrane are presented in the form of a new database called METPET. The information provides a tool for the spatial analysis of metamorphic assemblage data, and for comparing metamorphic facies with other geological, structural, or geochemical data. The data are used to present revised metamorphic grade maps for this part of the Eastern Goldfields Granite–Greenstone Terrane. The resulting patterns largely conform to those of earlier studies, but highlight the lack of close association between regional metamorphism and granitoids emplaced during D_1 compression deformation (pre-regional folding). This study also highlights a northwest trend of discontinuous metamorphic highs. Extending from southeast of Kambalda to the Scotia–Kanowna batholith, this trend is probably associated with the continuation at depth of a ridge of granitoids emplaced during late D_2–D_3 deformation (post-regional folding). Wide areas of biotite-absent pelitic and quartzofeldspathic rocks are spatially associated with fault zones or tectonized stratigraphic contacts, and probably result from widespread and pervasive alteration. Similar to previous studies, this study shows that the regional distribution of metamorphic facies cuts across domain and terrane boundary faults; however, conclusive evidence for areas of prehnite–pumpellyite or zeolite facies has not been found. The low-pressure, facies-series metamorphism of the Kalgoorlie region may be a consequence of the magmatic heat advection produced by the series of granitoid intrusions that traverse the region.

KEYWORDS: metamorphism, petrography, metamorphic assemblage, metamorphic facies, Kalgoorlie, Eastern Goldfields, METPET, spatial data, granitic rocks

Introduction

Regional metamorphic patterns provide information critical to the interpretation of the thermal and tectonic evolution of metamorphosed terranes (e.g. Spear, 1993). Despite this, few studies of metamorphic-grade distribution within the greenstones of the Yilgarn Craton have been reported. The primary sources of information are Binns et al. (1976; Eastern Yilgarn Craton), Ahmat (1986; Southern Cross 'Province'), and Dalstra et al. (1999; Southern Cross and Diemals 'Belts'). Groenewald et al. (2000) presented a metamorphic facies map of the Menzies to Norseman section of the Eastern Goldfields Granite–Greenstone Terrane, based on data from Binns et al. (1976), Swager et al. (1990, 1995), Witt (1993a), Swager (1995), and Wyche (1998). However, there has been little work specifically aimed at defining metamorphic patterns within the central parts of the late Archaean greenstones in the Kalgoorlie region since the work of Binns et al. (1976). This Record provides an updated metamorphic map and petrographic database for a 20 000 km^2 area coverering much of the Kalgoorlie region of the Eastern Goldfields Granite–Greenstone Terrane.

Re-examination of the metamorphic patterns in the Kalgoorlie region has become necessary for a number of reasons. Since the study of Binns et al. (1976), extensive

[1] E. & J. Mikucki Geological Consultants, 2285 Coolgardie Street, Mundaring, W.A. 6073

1:100 000-scale mapping has greatly increased our knowledge of the southern Eastern Goldfields (see Groenewald et al., 2000). Seismic (Goleby et al., 1993), gravity (Bell et al., 2000), and other geophysical data have extended our knowledge of the structure of the greenstones into the third dimension (see models presented in Swager et al., 1997 and Archibald, 1998). This has led to a better understanding of the tectono-stratigraphic evolution of the Kalgoorlie region (Swager, 1997). Refinement of metamorphic-grade patterns is the first step towards comparable advances in understanding the tectonothermal evolution of the southern Eastern Goldfields. The Kalgoorlie region is also host to some significant gold deposits, including those at Mount Charlotte, the Golden Mile, Kanowna Belle, St Ives, and Coolgardie. Because the origin, evolution, and migration of the gold-related hydrothermal fluids are intimately associated with the thermal evolution of the Eastern Goldfields (Groves and Phillips, 1987; Witt, 1993b), metamorphic grade is an important constraint on ore genesis.

One great advantage of this study over all previous metamorphic studies of the region is that locality and metamorphic-assemblage data for each sample are recorded in a database that is accessible through a Geographical Information System (GIS). Thus additional entries to the database can be included once the information becomes available. More importantly, individual data points can be plotted along with metamorphic zone or facies boundaries, allowing direct comparison between these boundaries and the constraining data. It also allows users to devise their own criteria for defining metamorphic zones or facies, if required.

The CD-ROM accompanying these notes contains the METPET database and the files necessary for viewing the data in a GIS environment (Appendix 1); a self-loading version of the GeoVIEWER.WA software package is also included.

Location

The area investigated (Fig. 1) is centred on Kalgoorlie and covers much of the south-central part of the Eastern Goldfields Granite–Greenstone Terrane between latitudes 30°12' and 31°27'S and longitudes 120°45' and 122°28'E (about MGA 284000 – 448000E, 6520000 – 6660000N). The area includes parts of the KALGOORLIE, KURNALPI, BOORABBIN, and WIDGIEMOOLTHA* 1:250 000 sheets. It is bound to the west and southwest by the Ida Fault and granitoids of the Burra Monzogranite Suite (Hunter, 1991), and to the north by the Mount Pleasant and Scotia–Kanowna batholiths and the Donkey Rocks and Menangina monzogranites (Witt and Davy, 1997; Fig. 2).

Geology and mineralization

The Kalgoorlie region forms part of the Eastern Goldfields Granite–Greenstone Terrane of the Archeaean Yilgarn Craton, and has been subdivided into a series of terranes and domains (Swager and Griffin, 1990; Swager et al., 1990, 1995; Swager, 1995, 1997) based on lithostratigraphic packages bound by regional faults and shear zones (Fig. 3). The geology of the study area is presented in Figure 4 and has been summarized by Swager et al. (1990, 1995), Swager (1995, 1997), Witt and Davy (1997), Groenewald et al. (2000), and Brown et al. (2001). A timeline for the geological history of the Kalgoorlie region is shown in Figure 5.

Linear greenstone belts and juxtaposed granites and gneisses form a pronounced north-northwesterly structural grain in the area that is defined by elongate granitoid bodies and the orientation of regional shear zones, lithostratigraphic contacts, and the regional metamorphic foliation. The greenstones comprise a lower mafic–ultramafic volcanic succession of metamorphosed basalts, komatiites, and mafic to ultramafic intrusive bodies, overlain by a felsic volcaniclastic and siliciclastic metasedimentary rock succession (Griffin, 1990). Both successions are unconformably overlain by polymict conglomerate and sandstones (e.g. the Penny Dam Conglomerate — Swager, 1994; the Merougil Beds — Griffin, 1990; and the Kurrawang Formation — Witt, 1994) thought to have been deposited in either localized, extensional syntectonic basins (Swager, 1997) or within more-regionally extensive sedimentary basins as submarine-fan and braided-river deposits (Krapez et al., 1997; Brown et al., 2001). Deposition of the earlier mafic–ultramafic and felsic volcanic–volcaniclastic successions occurred between c. 2720 and c. 2675 Ma, whereas a minimum age of c. 2660 Ma for the overlying conglomeratic units has been suggested (Nelson, 1997).

The deformation history of the Kalgoorlie region is complex. Commonly recognized elements include early north-directed, D_1 recumbant folding and thrusting, D_2 large-scale, upright folding, D_3 north-northwesterly trending strike-slip faulting and associated folding, and continued D_4 shortening. A number of less-understood extensional deformation events have also been proposed, including post-D_3 extensional collapse of the entire Eastern Goldfields fold-and-thrust belt (Hammond and Nisbet, 1992; Swager, 1997; Swager and Nelson, 1997; Witt and Davy, 1997).

Granitoid plutonism within the terrane occurred over an extended time period. Witt and Swager (1989), Champion and Sheraton (1993), and Witt and Davy (1997) recognized two main episodes of granitoid magmatism. Pre-regional folding granitoid complexes, such as the Mount Pleasant and Scotia–Kanowna batholiths (Fig. 2), form composite, elongate domes in the core of F_2 anticlines. Witt and Davy (1997) considered that these were emplaced as broadly conformable, sheet-like bodies at or near the base of the exposed greenstone sequences during D_1 compression. The pre-regional folding granitoid complexes contrast with circular to ovoid post-regional folding granitoids. A third granitoid group, granitoid gneiss, is present on the southwestern margin of the study area. Witt and Davy (1997) stated that available data indicate that the gneiss is deformed and metamorphosed pre-regional folding granitoid. Geochemical classifications for granitoids in the Eastern Goldfields Granite–

* Capitalized names refer to standard 1:250 000 map sheets

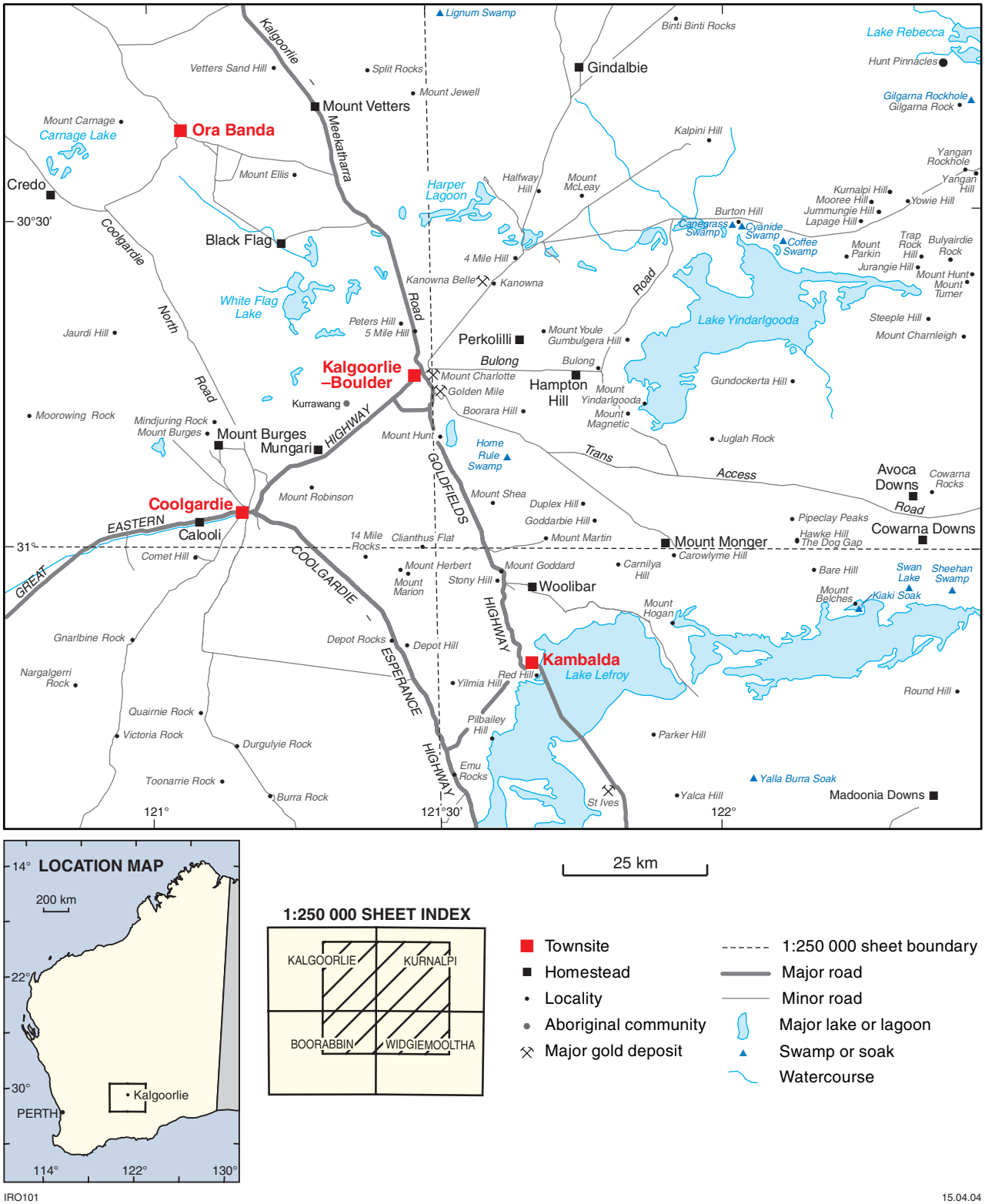

Figure 1. Locality map of the study area in the Kalgoorlie region

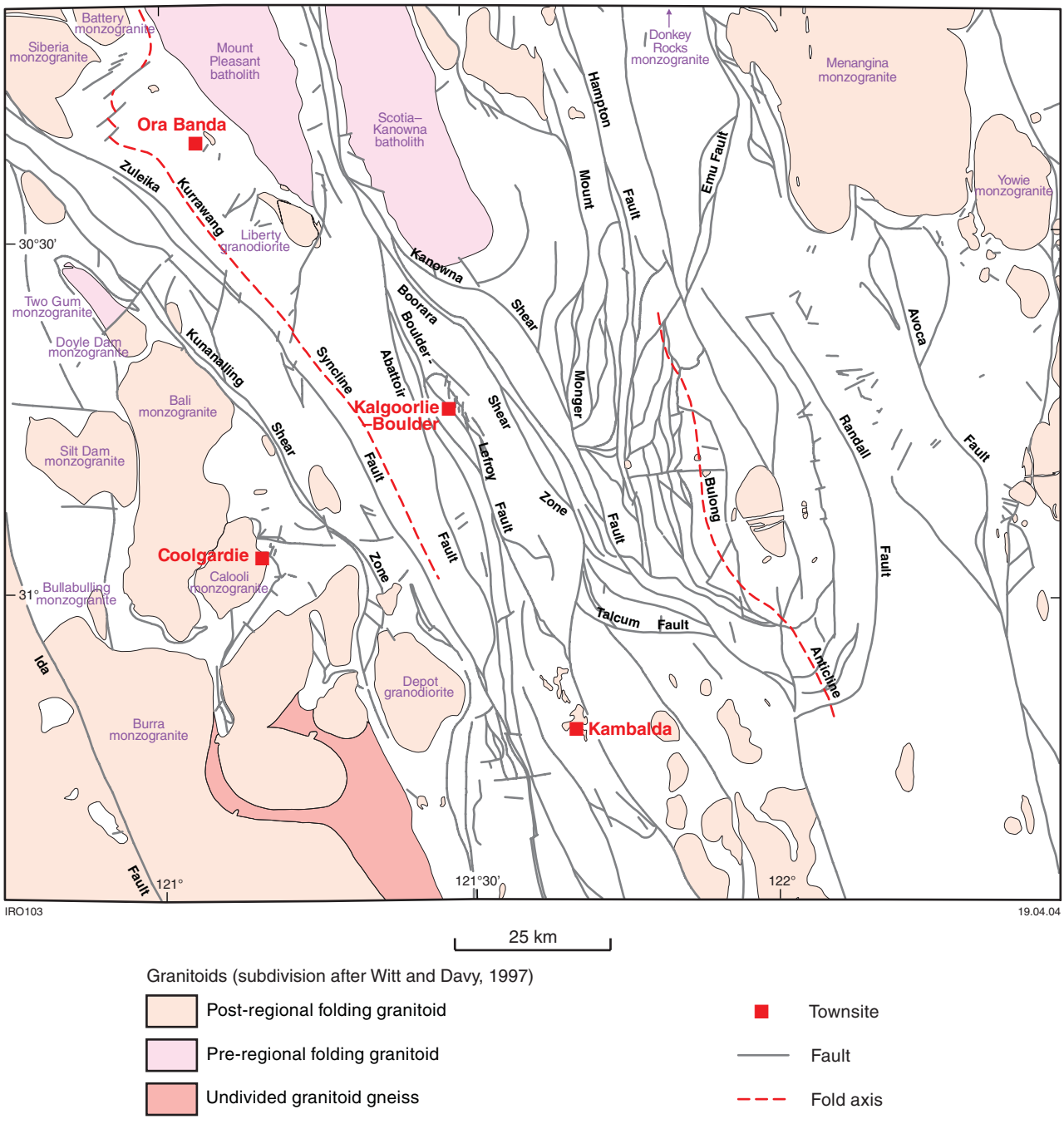

Figure 2. Granitoid intrusions and major structures in the Kalgoorlie region (after Vanderhor and Flint, 2001)

Greenstone Terrane have been put forward by Champion (1997) and Champion and Sheraton (1997). These latter works recognize two dominant groups (high-Ca and low-Ca) and three minor groups (high-HFSE*, mafic, and syenitic) of granitoids.

Recent geochronological data suggest that there is no simple relationship between structural history, geochemistry, and age. Inconsistencies include younger, strongly deformed granitoid and gneiss (2.65 – 2.64 Ga), and older, nonfoliated granitoids (2.68 – 2.65 Ga; Brown et al., 2001). Granitoid age data summarized by Brown et al. (2001) indicate an apparent continuum between c. 2.7 and 2.63 Ga, with a pronounced peak around 2.67 – 2.65 Ga. The peak metamorphic conditions are considered to correspond to late D_2–D_3 deformation, and were contemporaneous with broadly syn-D_3 granitoid emplacement (Brown et al., 2001).

The Kalgoorlie region contains significant gold and nickel deposits. The Golden Mile is the largest gold deposit, with well over half the total gold production for the region. The Kambalda nickel deposits are the premier nickel sulfide occurrences in Australia, and have produced most of the historical nickel production for the region.

* high field-strength elements

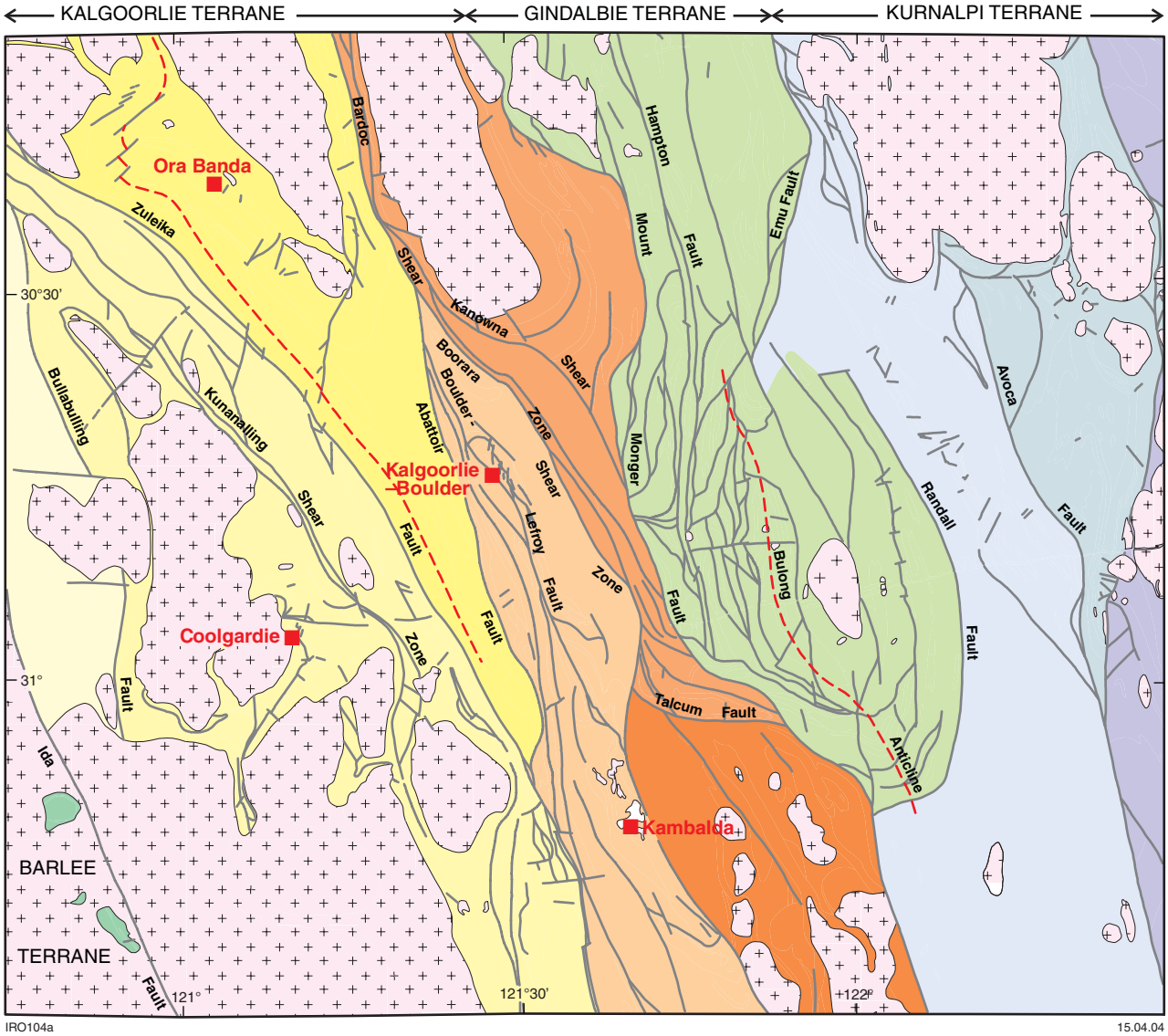

Figure 3. Major tectono-stratigraphic domains of the Kalgoorlie region (modified from Swager and Griffin, 1990; Swager et al., 1990, 1995; Swager, 1995, 1997)

On a regional scale, all lithologies in Archaean greenstone belts may be mineralized with respect to gold (Solomon and Groves, 1994); however, in the Kalgoorlie region most of the significant gold deposits are hosted by rocks of mafic composition, with metabasalt and metagabbro the common host rocks. The notable exception is the Kanowna Belle deposit, which is hosted by porphyry and felsic metavolcanic rocks. The majority are structurally controlled, mesothermal lode deposits of gold-only type, associated with distinctive wallrock alteration haloes (Solomon and Groves, 1994). The Golden Mile, Paddington, and New Celebration deposits and deposits in the St Ives area are adjacent to regional-scale deformation zones. On a mining district scale, gold

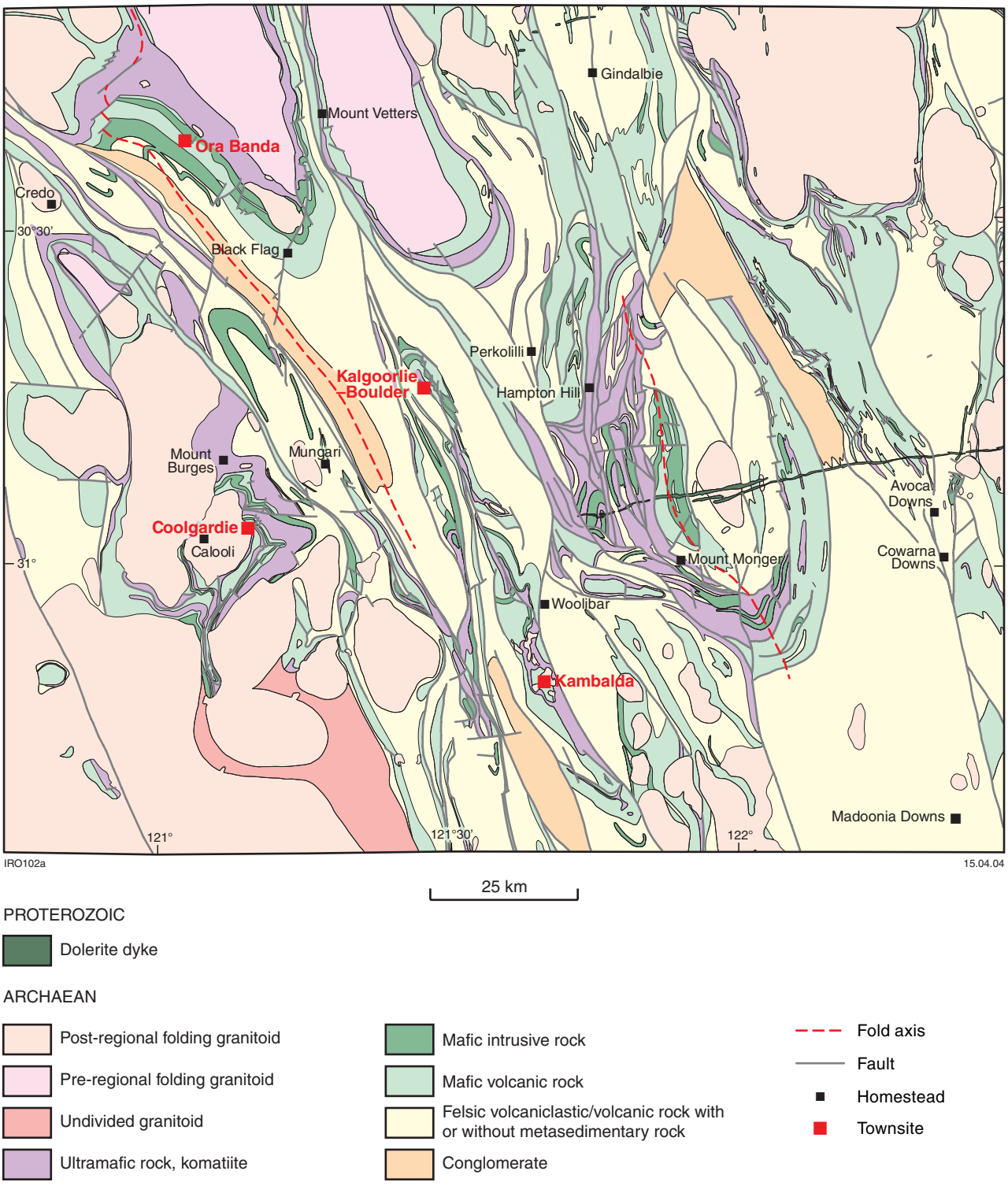

Figure 4. Precambrian geology of the Kalgoorlie region (after Vanderhor and Flint, 2001)

mineralization may exist in crosscutting or layer-parallel shear zones (e.g. the Golden Mile deposit), strike-extensive laminated quartz veins (e.g. Kundana), and quartz-vein arrays (e.g. Mount Charlotte and Paddington; Solomon and Groves, 1994). Solomon and Groves (1994) noted that the metamorphic setting of Archaean gold deposits ranges from subgreenschist to granulite facies, and the metamorphic P–T regime corresponds broadly to the brittle–ductile transition.

Metasomatic wallrock or hydrothermal alteration associated with gold involves the introduction of CO_2, K_2O, S, and H_2O, and the more localized introduction of Na_2O or CaO (Solomon and Groves, 1994). SiO_2 has been either introduced or redistributed (Solomon and Groves, 1994). The mineralogical expression of metasomatism reflects the composition and metamorphic grade of the host rock (Mueller and Groves, 1991; Witt, 1993a,b). Witt (1993a) concluded that alteration assemblages within particular rock types are controlled on a regional scale by temperature, which in turn correlates broadly with metamorphic grade.

Metakomatiite is the host rock for most of the stratiform nickel ores in the region. The present mineralogy is a function of the original bulk composition, metamorphic grade, and the X_{CO_2} of metamorphic or pre-metamorphic fluids, or both (Solomon and Groves, 1994).

Sample coverage

This study is based on petrographic descriptions of thin sections from the Geological Survey of Western Australia (GSWA) collection. A total of about 2000 descriptions are currently contained in the METPET database. About 75% of the descriptions are by E. J. Mikucki, and the bulk of the remainder is taken from the earlier work of R. K. Fagan (Fagan, 1998). Some descriptions by W. K. Witt (Witt, W. K., 1997, written comm.) are also included. Spatial data for the GSWA samples are from the GSWA WAROX database. Figure 6 shows the location of all thin sections listed in the METPET database. Except for areas underlain by granitoids, few regions lack sample coverage. Thin-section localities for which petrography is available are most abundant in the eastern half of the study area, beyond about 121°26'E (MGA 350000E). Sample density is lowest in the central parts of the study area, roughly between the Kunanalling Shear Zone and Mount Monger Fault at latitudes between Kalgoorlie and the New Celebration gold mine. Nevertheless, the overall spatial coverage of the study area is reasonably good, allowing most metamorphic isograds for the common rock types to be relatively well constrained on a regional basis. Isograds based on less-common rock compositions (e.g. pelitic and semipelitic rock types) are, understandably, less well constrained.

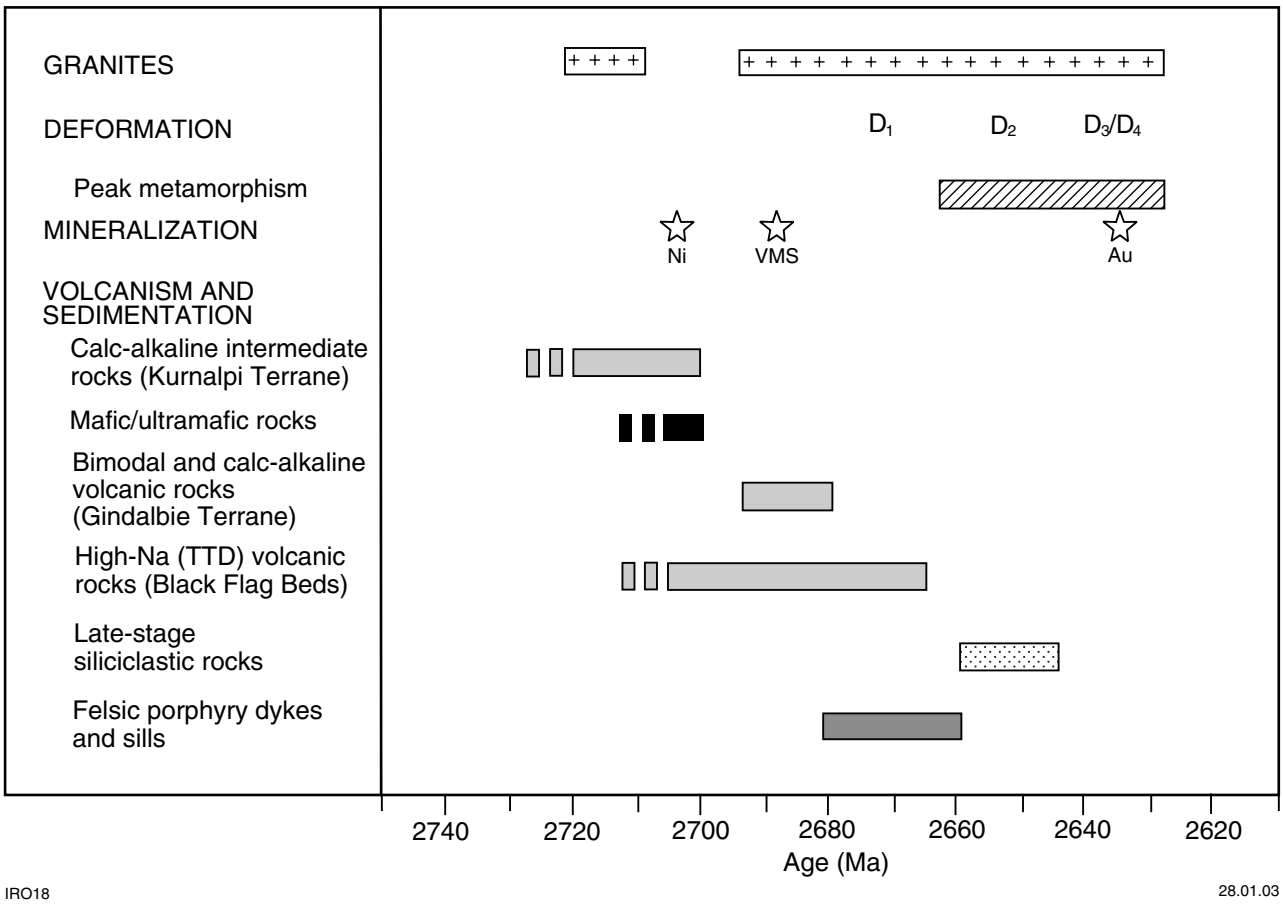

Figure 5. Time–event summary of the geological history of the Kalgoorlie region (modified from Brown et al., 2001). VMS: volcanogenic massive sulfide; TTD: trondhjemite–tonalite–dacite

METPET database

Petrographic descriptions of the rocks examined in this study are tabulated in the METPET database. The database format accommodates a number of characteristics that can be used to classify both the style of metamorphism (Binns et al., 1976) and metamorphic grade. Each entry is described by up to 20 individual data fields, which can be broadly grouped into three different types (Table 1). Sample-identity and spatial-data fields include those for the GSWA sample number (plus a separate field for a suffix, if required), geographical and MGA coordinates, and the petrographer. Fields that hold primary observational data include those describing the metamorphic style, IUGS Subcommission on the Systematics of

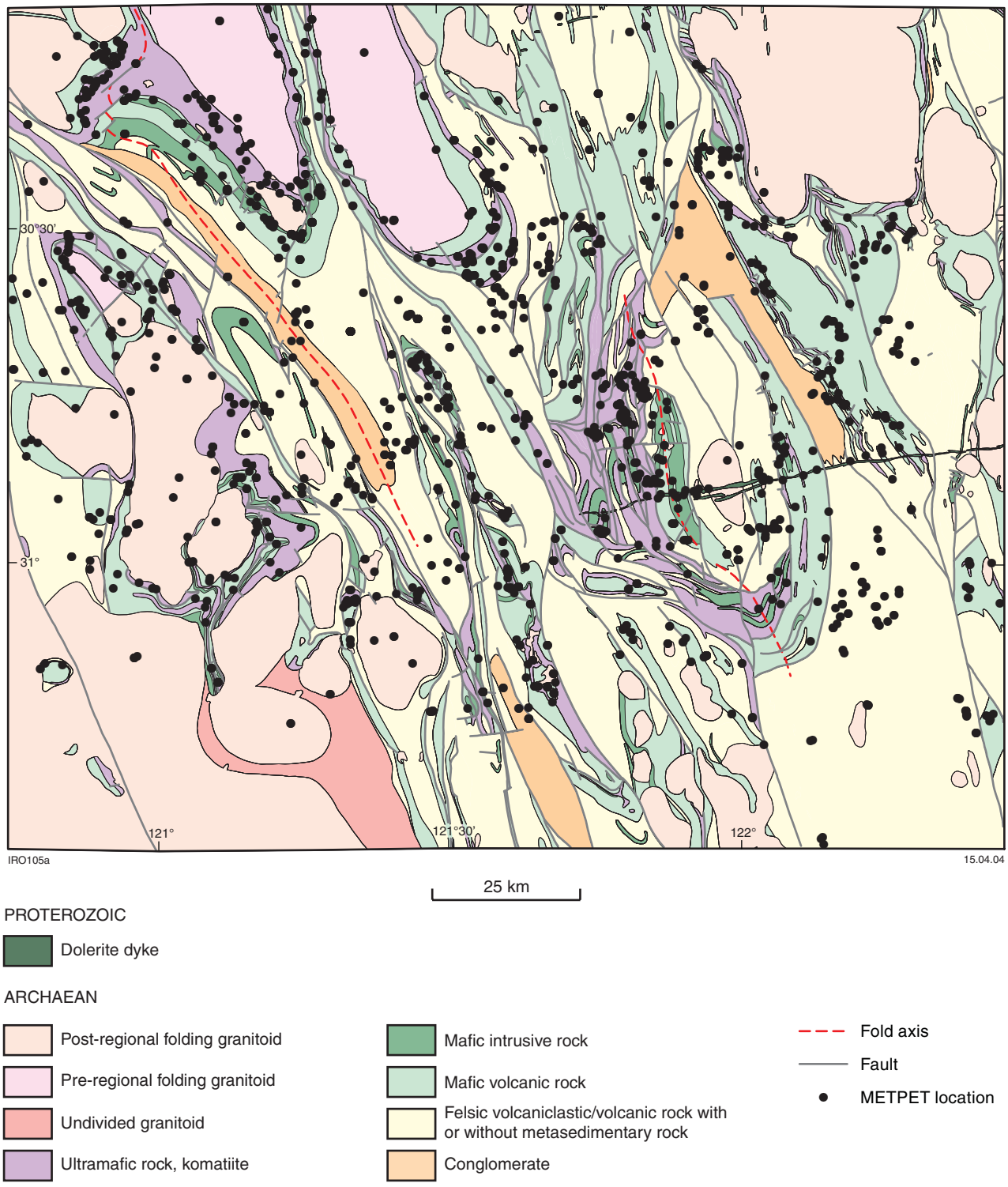

Figure 6. Locality map for all thin-section samples described in this study (geology after Vanderhor and Flint, 2001)

Table 1. Data fields in the METPET database

Sample-identity and spatial-data fields
GSWA Sample Number
MGA zone
Easting
Northing
Latitude
Longitude
Petrographer
Primary-observational-data fields
Prograde assemblage
Plagioclase composition
Amphibole type and whether coexisting amphiboles are present
Metamorphic style ('static' or 'dynamic' as defined by Binns et al., 1976)
SCMR root name
Extent of recrystallization
Degree of strain (deformation intensity)
Retrograde assemblages
Hydrothermal assemblages
Relict primary phases
Comments
Interpretive-data fields
Protolith group
Metamorphic facies
Metamorphic zone
Rock name

Metamorphic Rocks (SCMR) root name, and the extent of recrystallization, as well as the prograde metamorphic mineral assemblage. There are also fields for recording retrograde metamorphic and hydrothermal mineral assemblages, deformation (degree of strain), relict primary phases, and short comments. The fields for interpretive data include rock name, original protolith type, metamorphic zone (if relevant), and interpreted metamorphic facies.

Primary observational data

Thin-section observations are listed in a number of data fields that record the prograde metamorphic assemblage and additional data on the style of metamorphism and nature of retrograde metamorphic or hydrothermal overprints (see Table 1). In general, minerals are listed according to their importance when defining peak metamorphic zone assemblages (see **Metamorphic zone codes**), rather than in terms of modal abundance. Minor minerals (generally less than 3–5 volume %) are enclosed in parentheses. Opaque minerals could only be unambiguously identified in special circumstances because the large majority of thin sections examined have cover slips. In cases where the crystal habit of the opaque mineral is diagnostic, such as ilmenite, a tentative identification of the opaque mineral is indicated in parentheses. Plagioclase composition and amphibole type are given separate fields in the database due to their importance in defining metamorphic zones for mafic rock types. The typical fine-grained nature of metamorphic plagioclase and scarcity of twinning means that plagioclase compositions can only be determined approximately, if at all. Therefore, in the database, plagioclase is classified as either sodic (albite) or calcic (oligoclase–anorthite), based on a combination of refractive indices comparisons, the Michel–Levy extinction method, and optic-sign determinations. Likewise, calcic amphiboles were grouped into actinolitic amphiboles, blue-green 'hornblendes', and green or green-brown hornblendes, based on their pleochroic colours in plane-polarized light. These terms are probably equivalent to the actinolite, 'pale' hornblende, and 'dark' hornblende reported by Binns et al. (1976), and are typical of the types of amphiboles recorded from metamorphosed mafic rocks elsewhere (e.g. Miyashiro, 1973; Yardley, 1989). As mineral identification is based on optical properties only, without chemical analyses, it is not possible to precisely identify the amphiboles. The terms 'actinolitic amphiboles' and 'hornblende' are used as general terms following the recommendation of Leak (1978) on the nomenclature of amphiboles. For rocks that have undergone intense and pervasive hydrothermal alteration or weathering, peak metamorphic mineralogy may be impossible to determine. In such cases, the prograde-assemblage field was left empty.

In addition to mineral assemblages and composition data, a number of fields in the database record information on the style of metamorphism. Binns et al. (1976) classed metamorphic rocks with penetrative, strong tectonic fabrics as 'dynamic', and metamorphic rocks with no penetrative fabrics and pre-metamorphic textures abundantly preserved as 'static'. These terms have been superceded by the nomenclature of SCMR, but have been included in the database for completeness and because of their common useage in the Eastern Goldfields literature. For the nomenclature scheme of SCMR, Schmid et al. (2002) proposed that the common metamorphic rocks be divided into three major groups on the basis of their structure. The database has a field containing the root names schist, gneiss, or granofels: a schist is a metamorphic rock that has a well-developed schistosity; a gneiss is a metamorphic rock where the schistosity is either poorly developed, or if well developed, is in broadly spaced zones; whereas if schistosity is effectively absent then the rock is termed granofels. Also recorded are the degree of textural modification (either partial or total metamorphic, or hydrothermal recrystallization) and the degree of strain. The latter is reported using a relative scale from zero to three, and is based on the observations outlined in Table 2. Zones of contrasting metamorphic style or deformation intensity can therefore be plotted independently of metamorphic grade.

Interpretive data

This section describes those fields that are interpretive in nature, including the rock name, the type of rock prior to metamorphism (protolith group), and the metamorphic facies and zone names. All are based, to a large degree, on the mineral assemblages and textural relationships summarized by the observational-data fields, and on user definitions of facies boundaries and metamorphic-zone assemblages. Only the protolith-group, metamorphic-zone, and metamorphic-facies fields warrant detailed discussion. The database contains both metamorphosed and unmetamorphosed rock types, and as a consequence the common practice of omitting the prefix 'meta-' in naming the meta-

Table 2. Qualitative strain index used in the METPET database

Strain index	*Degree of strain*	*Typical textures*
0	unstrained rock	Original textures preserved or recrystallized. Decussate fabric
1	weak deformation	Weak spaced-cleavage or foliation generally formed by pressure solution and marked by trails of residual mineral concentrations (may be styolitic), little to no grain flattening or preferred alignment
2	moderate to strong deformation	Strong anastomosing or penetrative foliation and grain alignment, moderate grain flattening, pressure shadows and transposition of primary structures and/or veins
3	intense deformation	Pronounced penetrative foliation and/or lineation, pronounced grain-flattening fabric, few unrecrystallized grains, well-developed metamorphic differentiated layering

morphosed lithologies is not followed in this study. The naming convention used follows the recommendations of the IUGS SCMR (Schmid et al., 2002).

Protolith groups

Rocks are categorized into a number of protolith groups based on the likely nature of their pre-metamorphic rock type. For samples from low-strain domains, the preservation of primary textures is good, and the nature of the rock prior to metamorphism can be determined relatively accurately. In higher strain domains, textural preservation is poorer and the nature of the protolith was determined primarily from mineral assemblage criteria. In the latter case, names for the protolith group are less specific (e.g. 'ultramafic rock' rather than komatiite). The groups are listed in Table 3. For the purpose of defining metamorphic facies and zone names (see below), the protolith groups are further divided into major rock-composition groupings. Protoliths of the same major rock-compositional grouping will develop similar metamorphic assemblages during prograde metamorphism, even though they may have very different geological origins.

Treatment of metamorphic facies and zones

Treatment of metamorphic grade in this work is based on the metamorphic-facies boundaries depicted in Spear (1993; Fig. 7), rather than on the domain terminology and boundaries of Binns et al. (1976). Most of the earlier work was carried out prior to consensus being reached on facies classification. Since that time, metamorphic facies have become widely accepted as a convenient way to convey approximate metamorphic grade, and are preferred here. This study also differs from Binns et al. (1976) in that the metamorphic boundaries portrayed in this Record are true mineral isograds, in that they represent boundaries between domains characterized by different index minerals or mineral assemblages in specific rock types. This is accommodated in the database by a field for metamorphic zone code (see below). In contrast, Binns et al. (1976) and subsequent workers plotted metamorphic domain boundaries (roughly analogous to metamorphic facies boundaries), and although this is a legitimate approach, the basis for a specific domain boundary remains somewhat ambiguous because domains are defined using assemblages from all major rock types. As shown below, the same information can be portrayed using mineral isograds without ambiguity as to what mineral assemblages are defining the boundary.

Table 3. Protolith groups

Ultramafic rocks (Um)
ultramafic rock
dunite/peridotite
pyroxenite/peridotite
komatiite
lamprophyre

Mafic rocks (B)
high-Mg or komatiitic mafic rock
tholeiitic mafic rock
unspecified mafic/intermediate volcanic rock

Quartzofeldspathic rock types (Qf)
granitoid
felsic volcanic rock
psammitic rock

Pelite and semipelitic rocks (P)
pelite and semipelite

Additional rock types
banded iron-formation
Fe-shale
calc-silicate rock
metamorphosed advanced argillically altered rock

Others
?(protolith unknown)
unsuitable or damaged section
sample is too weathered

NOTE: The codes in parentheses are those used to indicate major rock composition groupings in metamorphic zone codes (see text)

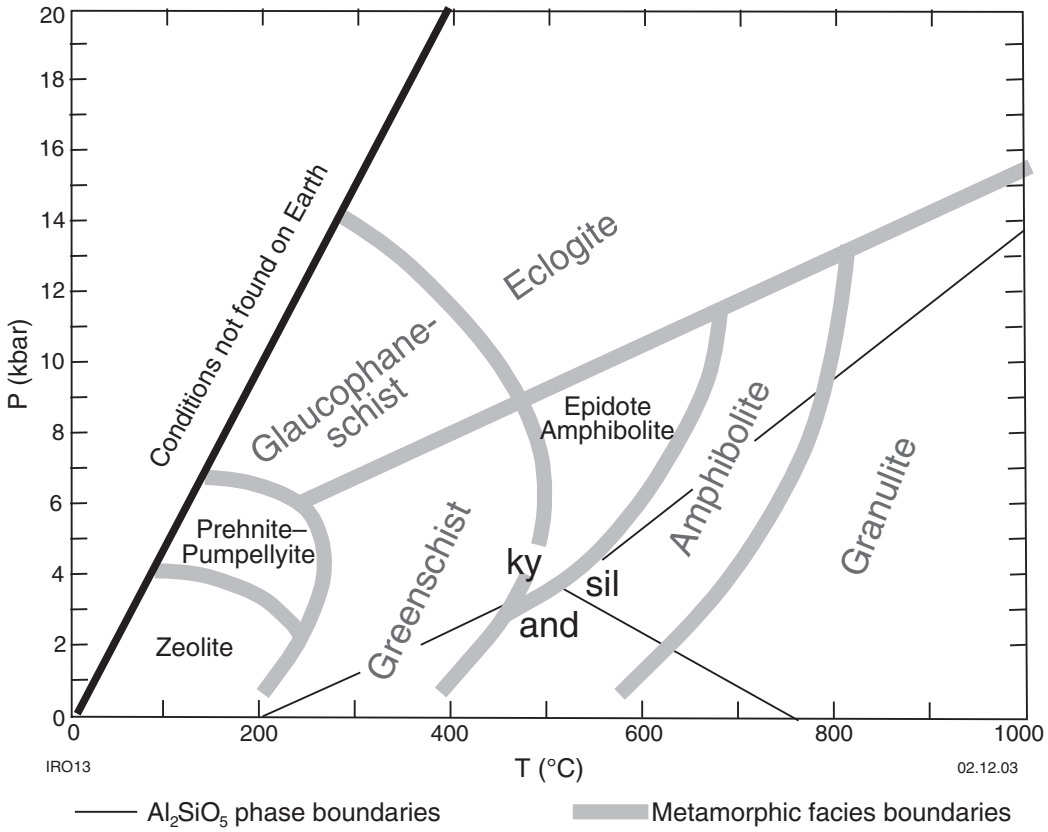

Figure 7. P–T diagram showing Al_2SiO_5 phase boundaries and the boundaries of the principal metamorphic facies types (after Spear, 1993). See Table 6 for mineral abbreviations

Metamorphic zone codes

The metamorphic zone codes (Table 4) convey information about the bulk rock composition and nature of the metamorphic assemblage for a specific sample, and are used to sort samples for creating metamorphic zone maps. Ideally, samples with the same zone code share the same broad bulk composition and critical index mineral (or minerals), and are assumed to have been metamorphosed at similar metamorphic grade. Because many samples do not contain diagnostic mineral assemblages, zone codes were not entered for all samples. Likewise, not all rock types were considered when assigning codes. For example, particular lithologies may be present in too few locations to be useful for mapping (e.g. banded iron-formation), or show conflicting or non-systematic spatial patterns when plotted on metamorphic grade maps (e.g. lizardite serpentinite versus antigorite serpentinite). Bulk rock composition codes are only presented for mafic, pelitic and semi-pelitic, and quartzofeldspathic rock types in the current version of the database. Highly aluminous schists, presumed to represent volcanic or ultramafic rocks that were argillically altered or weathered prior to metamorphism (Purvis, 1984), are also given codes because the metamorphic assemblages developed in these rocks provide useful constraints on metamorphic grade.

It is important to note that the metamorphic zone codes, as defined here, are specific to the project area and do not necessarily equate to zonal sequences documented elsewhere (e.g. Harte and Hudson, 1979; Yardley, 1989). In many cases, the specific assemblages used to define metamorphic zones in other geological settings are absent in the Kalgoorlie area due to differences in metamorphic field gradients. In other cases, the specific bulk rock compositions that develop the key assemblages are sparsely distributed in the Eastern Goldfields. Thus, for example, garnet and staurolite zones were not included in the present scheme for pelitic rocks because only three localities (two of which are in close proximity to each other) contain rocks with the appropriate compositions to form these assemblages. Likewise, similar metamorphic zone codes for different bulk rock compositions (e.g. chlorite zones for pelites, quartzofeldspathic rocks, and mafic rocks — $P_{(chl)}$, $Qf_{(chl)}$, and $B_{(chl–mu)}$ respectively) do not necessarily mean that each was metamorphosed at the same metamorphic grade, even though they may share common metamorphic minerals.

Witt (1993a) found that hydrothermal alteration assemblages in the Eastern Goldfields vary systematically with metamorphic grade, and therefore can be treated in the same manner. Hydrothermal alteration assemblage codes for the major rock composition groupings are summarized in Table 5, and are based on the assemblages of Witt (1993b). The subscript ‘a’ following the bulk rock composition code indicates that the rock has been altered. In these cases, the mineral abbreviations in brackets (refer to Table 6) specify the hydrothermal alteration zone assemblage to which the sample belongs.

Table 4. Metamorphic zone codes for major bulk rock composition groupings

P *pelitic/semipelitic rocks*	*Qf* *quartzofeldspathic rocks*	*B* *mafic rocks*	*Al* *highly aluminous rocks*
chlorite – white mica (–K-feldspar), or chlorite–biotite(–K-feldspar) ($P_{(chl)}$: chlorite zone)	white mica – albite(–chlorite–tremolite–epidote) ($Qf_{(chl)}$: chlorite zone)	chlorite–albite(–epidote– white mica –carbonate) ($B_{(chl–ms)}$: chlorite greenschist)	white mica – andalusite(–chloritoid) or white mica – chloritoid–chlorite ($Al_{(cld–and)}$: chloritoid schists)
biotite – white mica (–chlorite) ($P_{(bt)}$: biotite zone)	biotite – white mica (–chlorite–tremolite–clinozoisite–hornblende–cordierite–albite or calcic plagioclase) ($Qf_{(bt)}$: biotite zone)	actinolite/tremolite–albite ($B_{(act–ab)}$: greenschists)	white mica – kyanite(–sillimanite–andalusite) ($Al_{(ky)}$: kyanite schists)
		actinolite/tremolite – calcic plagioclase ($B_{(act–pl)}$: calcic plagioclase greenschists)	
biotite–andalusite(–cordierite–staurolite) ($P_{(bt–and)}$: biotite–andalusite zone)		blue-green amphibole – albite(–epidote) ($B_{(bgamp–ab)}$: epidote amphibolites)	
		blue-green amphibole – calcic plagioclase ($B_{(bgamp–pl)}$: amphibolites)	
sillimanite(–biotite–cordierite) ($P_{(bt–sil)}$: biotite–sillimanite zone)		green hornblende – calcic plagioclase ($B_{(hbl–pl)}$: amphibolites)	
sillimanite–K-feldspar–quartz (–white mica) ($P_{(sil–kfs)}$: sillimanite–K-feldspar zone)			

NOTE: These metamorphic zone codes are only applicable for the low-pressure series in the Kalgoorlie region

Table 5. Hydrothermal assemblage codes for major bulk rock composition groupings

Ba *mafic rocks* *(after Witt, 1993b)*	*Pa* *pelitic/semipelitic* *rocks*	*Qfa* *quartzofeldspathic* *rocks*	*Uma* *ultramafic rocks* *(after Witt, 1993b)*
chlorite–albite–carbonate(–white mica) ($Ba_{(ank)}$: ankerite zone)	chlorite – white mica –carbonate(–albite) ($Pa_{(ank)}$: ankerite zone)	chlorite – white mica –carbonate(–albite) ($Qfa_{(ank)}$: ankerite zone)	talc–chlorite–carbonate(–sericite/fuchsite) ($Uma_{(tlc–chl)}$: talc–chlorite zone)
biotite–chlorite–carbonate(–white mica) (albitic or calcic plagioclase) ($Ba_{(bt)}$: biotite zone)	biotite–chlorite–carbonate(–white mica) (albitic or calcic plagioclase) ($Pa_{(bt)}$: biotite zone)	biotite–chlorite–carbonate(– white mica) (albitic or calcic plagioclase) ($Qfa_{(bt)}$: biotite zone)	biotite–amphibole ($Uma_{(bt–amp)}$: amphibole zone)
biotite–hornblende – calcic plagioclase (–carbonate) ($Ba_{(amp)}$: amphibole zone)	Ca-amphibole–plagioclase(–carbonate) ($Pa_{(amp)}$: amphibole zone)		
diopside–biotite–hornblende – calcic plagioclase ($Ba_{(di)}$: diopside zone)			
diopside–K-feldspar–hornblende– calcic plagioclase (–garnet) ($Ba_{(di–kfs)}$: diopside–K-feldspar zone)			

NOTE: These metamorphic zone codes are only applicable for the low-pressure series in the Kalgoorlie region

Where samples contain minor hydrothermal alteration, but peak metamorphic assemblages can still be discerned, zone codes reflect peak metamorphic minerals, although hydrothermal assemblages are also indicated in a separate data field. Samples that have been pervasively altered so that peak metamorphic assemblages cannot be distinguished are only given a hydrothermal alteration assemblage code. Again, letter codes for altered rocks do not correspond to the same assemblage in unaltered rocks. For example, biotite-zone metapelites ($P_{(bt)}$) and hydrothermally altered, biotite-assemblage metapelites ($Pa_{(bt)}$) differ (cf. Tables 4 and 5). Hydrothermal alteration associated with the major gold deposits in the Kalgoorlie region, based on a review of the literature, is presented in Appendix 2.

Metamorphic facies

A data field for the metamorphic facies type is also included in the METPET database. This provides a means of correlating metamorphic grade between rocks of differing bulk rock composition, and therefore characterized by different metamorphic mineral assemblages (e.g. Yardley, 1989). The samples so far included in the database range from lower greenschist facies through to lower granulite facies and define a low- to intermediate-pressure metamorphic-facies series (Fig. 7). Prograde assemblages of the zeolite and prehnite–pumpellyite facies have not been identified, although Binns et al. (1976) mapped domains equivalent to prehnite–pumpellyite and lower greenschist facies in the area. Prehnite and lawsonite have, however, been observed as post-metamorphic vein fill in rare cases. The following sections discuss the methodology used to assign facies types to samples in the database. Note that, again, not all samples contain assemblages amenable to constraining metamorphic grade. In these cases the facies may not be defined, and qualifiers (>, <, etc.) have been used to indicate minimum or maximum constraints on metamorphic grade. The database only provides facies types for the major bulk rock compositional groupings (mafic rocks, pelites and semipelites, quartzofeldspathic rocks, and ultramafic rocks) and for the highly aluminous kyanite and andalusite schists. Facies determinations for rock types other than the mafic rocks are based on the petrogenetic grids for pelitic and ultramafic rocks provided by Spear (1993) and Trommsdorf and Evans (1977). The grids, along with the relevant mineral compatibility diagrams for low-pressure metamorphism, are shown in Figures 8 to 10.

Table 6. Mineral abbreviations

Mineral name	*Abbreviation*
Al_2SiO_5 polymorphs	alsi
Actinolite	act
Albite	ab
Andalusite	and
Ankerite	ank
Anthophyllite	ath
Antigorite	atg
Biotite	bt
Blue-green amphibole	abamp
Brucite	brc
Calcite	cal
Chlorite	chl
Chloritoid	cld
Cordierite	crd
Diopside	di
Dolomite	dol
Enstatite	en
Forsterite	fo
Garnet	grt
Hornblende	hbl
K-feldspar	kfs
Kyanite	ky
Magnesite	mgs
Microcline	mc
Muscovite	ms
Plagioclase	pl
Pyrophyllite	prl
Quartz	qtz
Sillimanite	sil
Staurolite	st
Talc	tlc
Tremolite	tr

Pelites and semipelites

Pelitic and semipelitic rocks outcrop at relatively few locations in the Kalgoorlie region, but are important because their mineral assemblages can be tightly constrained in P–T space by phase equilibria (Fig. 8). Metamorphic facies for the pelitic rocks can therefore be used to better constrain the grade of spatially adjacent non-pelitic rocks. The boundary between chlorite- and biotite-zone pelites (the biotite isograd) has been used to define the boundary between lower and upper greenschist-facies conditions. This is consistent with common usage elsewhere (e.g. Miyashiro, 1973; Yardley, 1989; Spear, 1993). In the Kalgoorlie region, biotite-zone assemblages persist until at least the mid- to upper amphibolite facies. Mineral assemblages indicative of lower to mid-amphibolite-facies conditions in other geological settings are relatively rare in pelitic rocks in the area as a consequence of the low-pressure-type metamorphism that characterizes this terrane (Spear, 1993). Upper amphibolite-facies pelites are represented by stable biotite–andalusite(–cordierite), biotite–cordierite, and cordierite–andalusite assemblages that indicate temperature and pressure conditions were above the staurolite–chlorite and chlorite breakdown reactions in Figure 8. A biotite–staurolite(–andalusite–garnet–chlorite) assemblage represents mid-amphibolite facies in relatively iron rich pelites from the southeastern corner of the study area. Higher grade, upper amphibolite-facies, sillimanite-bearing rocks are also present. Two samples (GSWA 063528 and 106015) contain sillimanite–microcline–quartz assemblages indicative of the sillimanite–K-feldspar zone, and therefore most probably reached at least uppermost amphibolite-facies conditions.

Quartzofeldspathic rocks

Rocks of quartzofeldspathic composition include metamorphosed granitic rocks, intermediate to felsic volcanic

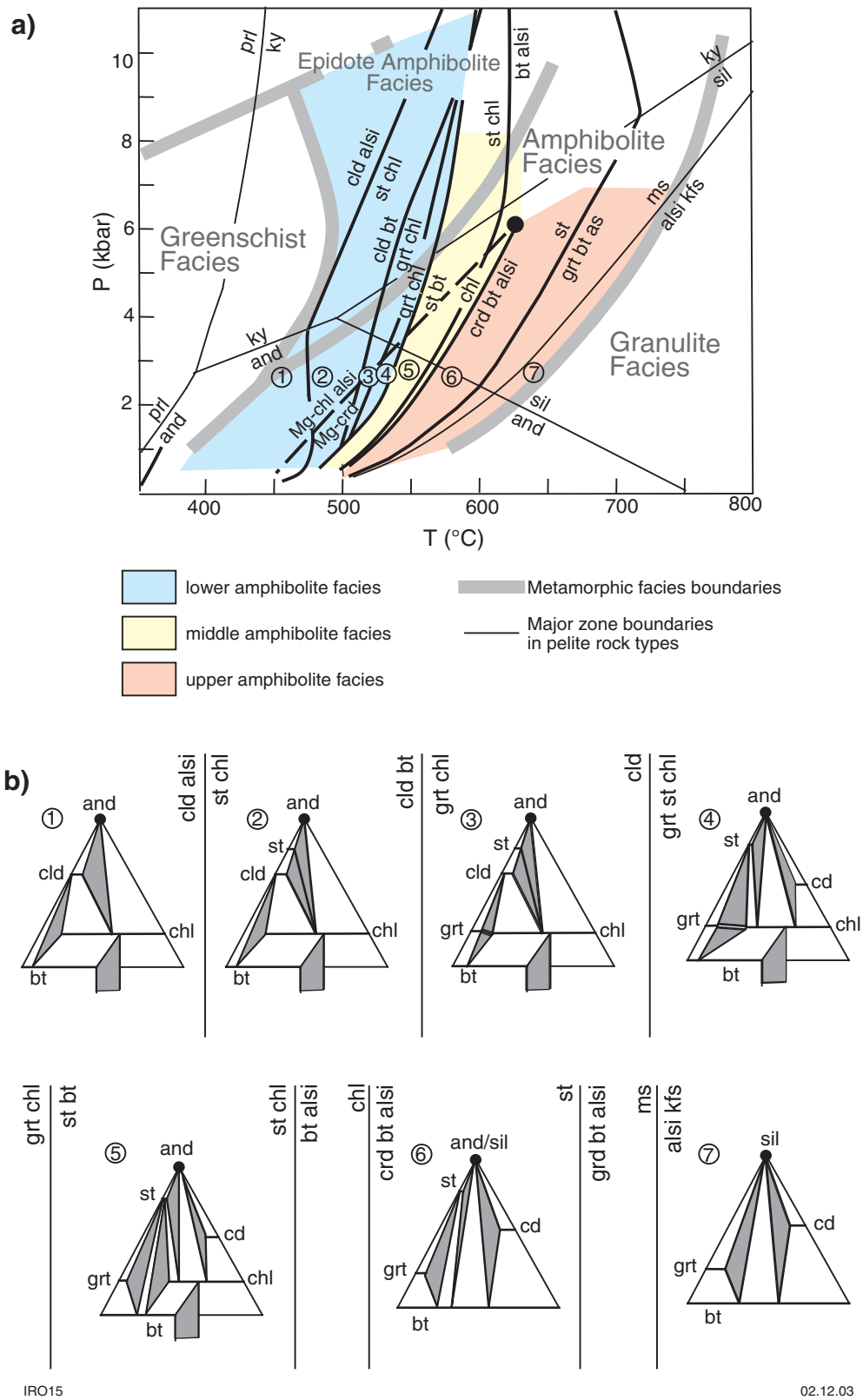

Figure 8. **a) Petrogenetic grid for pelitic rock types (muscovite+quartz+H_2O in excess) after Spear and Cheney (1989). Here the amphibolite facies have been subdivided into lower, middle, and upper amphibolite facies fields along reactions responsible for major zone boundary changes in pelitic rock types; b) Mineral compatibility (AFM) diagrams for the numbered points in a), summarizing the major mineral compatibility changes that occur during low-P–T facies metamorphism of pelitic rocks. See Table 6 for mineral abbreviations**

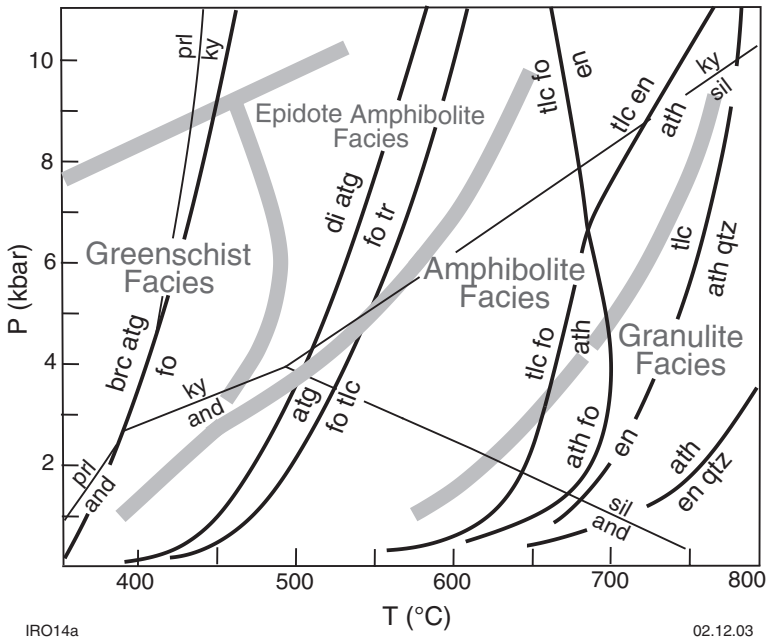

Figure 9. Petrogenetic grid for ultramafic rock types in the CO_2-free system (after Spear, 1993). Metamorphic facies boundaries are the same as in Figure 7. See Table 6 for mineral abbreviations

and volcaniclastic rocks, and psammitic rocks (including feldspathic sandstones). For the most part, the metamorphic mineral assemblages of these rock types are relatively insensitive to changes in metamorphic grade (Spear, 1993). Because of this, only chlorite- and biotite-zone assemblages could be distinguished. The biotite isograd in these rocks probably corresponds to a slightly different metamorphic reaction than that in the pelitic rock types (Mather, 1970), but is still indicative of the transition from lower to upper greenschist-facies conditions. Maximum metamorphic grades in the biotite zone for quartzofeldspathic rocks could, however, extend to at least amphibolite facies, as evident from minor amounts of hornblende or cordierite in some samples.

High-alumina rocks

Rare, highly aluminous kyanite and andalusite schists are described for several localities within the study region. Most contain chrome-bearing accessory minerals such as fuchsite (Cr-bearing white mica), and are thought to have formed by metamorphism of argillically altered or deeply weathered volcanic and ultramafic rocks (Purvis, 1984). Metamorphic assemblages vary from white mica – andalusite(–chloritoid) and white mica – chloritoid–chlorite assemblages near the Gordon–Sirdar mine, east of the Scotia–Kanowna batholith, to white mica – kyanite (–chloritoid–andalusite) assemblages in the Steeple Hill – Rocky Dam area (Swager, 1994), and kyanite(–sillimanite–andalusite)– white mica schists in the Mount Martin – Carnilya Hill region and along the southeastern limb of the Bulong Anticline. The assemblages developed in these rocks are indicative of moderate pressures (less than 4 kbar) and uppermost greenschist- to lower amphibolite- facies conditions (Fig. 8).

Ultramafic rocks

Ultramafic rocks within the study area consist dominantly of metamorphosed komatiite flows as well as dunite and peridotite cumulate rocks. The komatiites mainly consist of non-diagnostic tremolite–chlorite assemblages, and therefore are of little use in defining metamorphic grade. Most of the ultramafic cumulate rocks are dominated by antigorite(–lizardite)–talc–carbonate or antigorite(–lizardite)–tremolite–talc assemblages. These antigorite-bearing assemblages must have formed at or below lower amphibolite-facies conditions, above which antigorite breaks down to form forsterite–talc (Fig. 9). The predominance of antigorite, rather than lizardite, indicates that metamorphism occurred at or above mid-greenschist-facies conditions (e.g. Donaldson and Bromley, 1981). However, these common mineral assemblages provide few other constraints on metamorphic grade.

Metamorphosed ultramafic rocks of demonstrably lower, or higher, metamorphic grade than that discussed above are uncommon. In relatively few samples, phases indicative of lower greenschist- or subgreenschist-facies conditions (e.g. brucite, lizardite, and pyroaurite) have been tentatively identified. Lizardite showed conflicting or non-systematic spatial patterns when plotted on metamorphic-grade maps. Its presence in otherwise higher grade domains probably reflects its formation as a late retrograde or hydrothermal phase, rather than during peak metamorphism (McQueen, 1981). In this study, pyroaurite has been identified in one sample (GSWA 100869), and possible brucite was identified in only three ultramafic samples (GSWA 060930, 090006, and 093983). This probably reflects the absence of subgreenschist-facies domains in the study area. However, brucite can be difficult to identify in thin section and pyroaurite can be

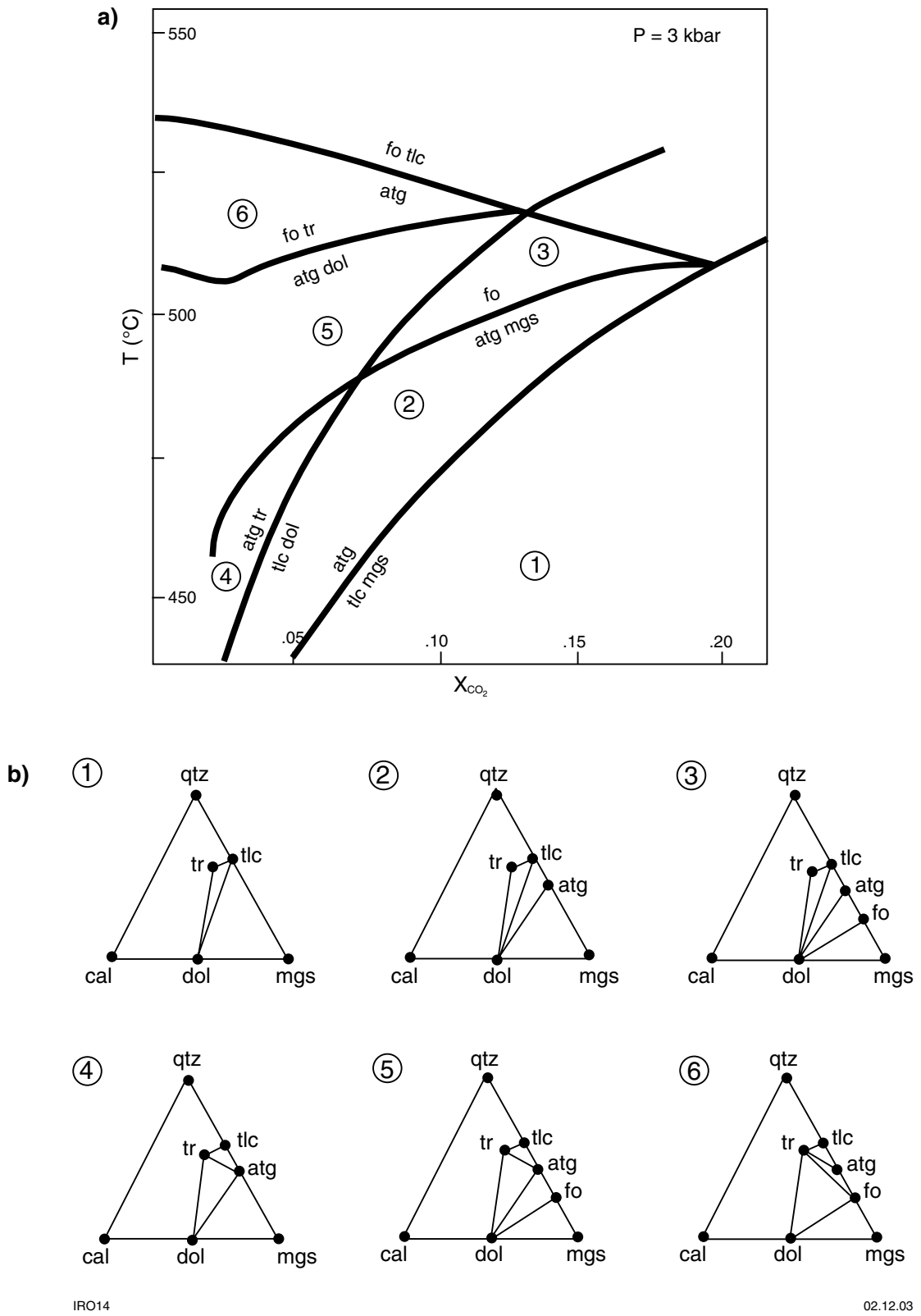

Figure 10. a) Petrogenetic grid for ultramafic rock types coexisting with CO_2–H_2O fluids at 3 kbar pressure (after Trommsdorf and Evans, 1977), and b) compatibility diagrams for the labelled isobarically divariant fields in a). See Table 6 for mineral abbreviations

absent or in low abundance in low-grade serpentinites (e.g. Donaldson, 1981). Thus their presence cannot be totally discounted without detailed X-ray diffraction and petrographic studies.

The forsterite–talc- and anthophyllite(–enstatite)-bearing assemblages of amphibolite facies metaperidotites are rare or absent in the samples examined. This probably reflects the fact that ultramafic rocks from the higher grade domains (e.g. adjacent to the Calooli and Bali monzogranites; see Fig. 2) are poorly represented in the database (Fig. 6).

The bulk compositions of many of the serpentinites in the Eastern Goldfields lie between forsterite and antigorite in the $MgO–SiO_2–H_2O$ ternary system (Donaldson, 1981); hence, the near absence of forsterite–antigorite serpentinites in the database, despite the presence of large domains of greenschist-facies rocks in the project area, requires explanation. One possibility is that low metamorphic temperatures or elevated X_{CO_2}, or both, during metamorphism prevented forsterite stability (Fig. 10). However, the predominance of talc–antigorite(–carbonate or tremolite) in these serpentinites favours another explanation. As indicated in Figure 10, the talc–antigorite assemblage is stable over the entire $T–X_{CO_2}$ space for which forsterite–antigorite is stable, but it requires lower $(Mg,Fe^{2+})O:SiO_2$ bulk compositions to form. Oxidation of ferrous iron-bearing minerals in the host ultramafic rocks could stabilize talc–antigorite over forsterite–antigorite assemblages by decreasing host-rock $(Mg,Fe^{2+})O:SiO_2$, thereby accounting for the observed rarity of metamorphic olivine in these rock types. This model is also supported by the high modal abundances of metamorphic magnetite in the serpentinites.

Mafic rocks

Metabasalts constitute a large proportion of the current database, commensurate with their abundance in the region and with their importance as a host rock for gold mineralization. This section summarizes the progressive mineralogical changes used in this study to define metamorphic-grade variations in these rocks. Most low-grade mafic rocks in the study area possess typical greenschist-facies mineral assemblages (actinolite–epidote – sodic plagioclase – chlorite). Zeolite minerals, prehnite, and pumpellyite are notably absent. A number of samples, however, lack actinolite and are composed mostly of chlorite–epidote– sodic plagioclase (–carbonate; less than 3–5 volume%). It is not certain in all cases whether this assemblage resulted from lowermost greenschist-facies metamorphism (Spear, 1993, p. 402), from weak, pervasive carbonate alteration, or from metasomatic changes to bulk rock composition during early sea-floor spilitization (e.g. Gelinas et al., 1982). In some cases, rocks with this assemblage are in close proximity to major shear zones (e.g. metabasalts next to the Boorara Shear Zone southwest of Kalgoorlie) and to rocks that are obviously altered. However, until more data become available, rocks with this assemblage are treated here as regionally metamorphosed, lowermost greenschist-facies rocks. Miyashiro (1973) noted that the first appearance of biotite in metabasites coincides with the biotite zone in metapelites in low-pressure-facies series metamorphism, but occurs at lower grades at higher pressures. Thus, the first appearance of biotite–muscovite in metabasalts is used as a provisional constraint on placement of a biotite isograd separating lower greenschist from upper greenschist rocks (see **Pelites and semipelites**).

At higher metamorphic grades, the transition between the greenschist- and amphibolite-facies mafic rocks is marked by the replacement of pale-coloured actinolite by blue-green amphibole (presumably hornblende) and by the change from sodic to calcic plagioclase in the mineral assemblages. In the study area, both transitions appear to be more or less at the same metamorphic grade, in that relatively few samples contain actinolite – calcic plagioclase or blue-green amphibole – sodic plagioclase assemblages. Furthermore, separate zones with these assemblages cannot be defined on metamorphic-grade maps. For the purposes of this study, the transition between upper greenschist and lower amphibolite facies is defined by the first occurrence of blue-green amphibole in mafic rocks (blue-green-amphibole isograd) because of the difficulties in obtaining accurate plagioclase compositions using optical methods. Chlorite and then epidote abundances also decrease significantly during transition from greenschist- to lower amphibolite-facies rocks.

Note that a distinct transitional zone of epidote amphibolites between greenschist- and amphibolite-facies metabasites has not been identified, even though rocks with blue-green amphibole – sodic plagioclase – epidote assemblages are present. On the contrary, mafic rocks with the assemblage blue-green amphibole – albite appear to coexist spatially with rocks where blue-green amphibole – calcic plagioclase is stable over wide areas in the southern and southwestern portions of the study area. Such a scenario could occur if metamorphism took place at pressures near the low-pressure terminus of the epidote-amphibolite field shown in Figure 10. Under such conditions small variations in bulk rock chemistry or pressure may be responsible for stabilizing epidote amphibolite over normal amphibolite-facies assemblages. It must also be acknowledged that the distinction between actinolites and hornblendes by optical microscopy is difficult and not always possible (e.g. Deer et al., 1966). Thus some of the metabasites tentatively identified as ‘epidote amphibolites’ in this study may yet turn out to be greenschists once quantitative mineral chemistry becomes available.

The change from blue-green amphibole to green or green-brown hornblende (green-hornblende isograd) is the next easily observable transition with increasing metamorphic grade. Metamorphic clinopyroxene may also be present with green hornblende in some rocks, but can also exist in rocks with blue-green amphibole. Mafic rocks of the green-hornblende zone are in close proximity to post-regional folding granitoids and cordierite-bearing biotite–andalusite-zone and biotite–sillimanite-zone metapelites. On this basis, they have been assigned an upper amphibolite-facies metamorphic grade. A single mafic-rock sample (GSWA 101128) contains both orthopyroxene and clinopyroxene. This sample is spatially adjacent to a large Proterozoic dyke and may represent

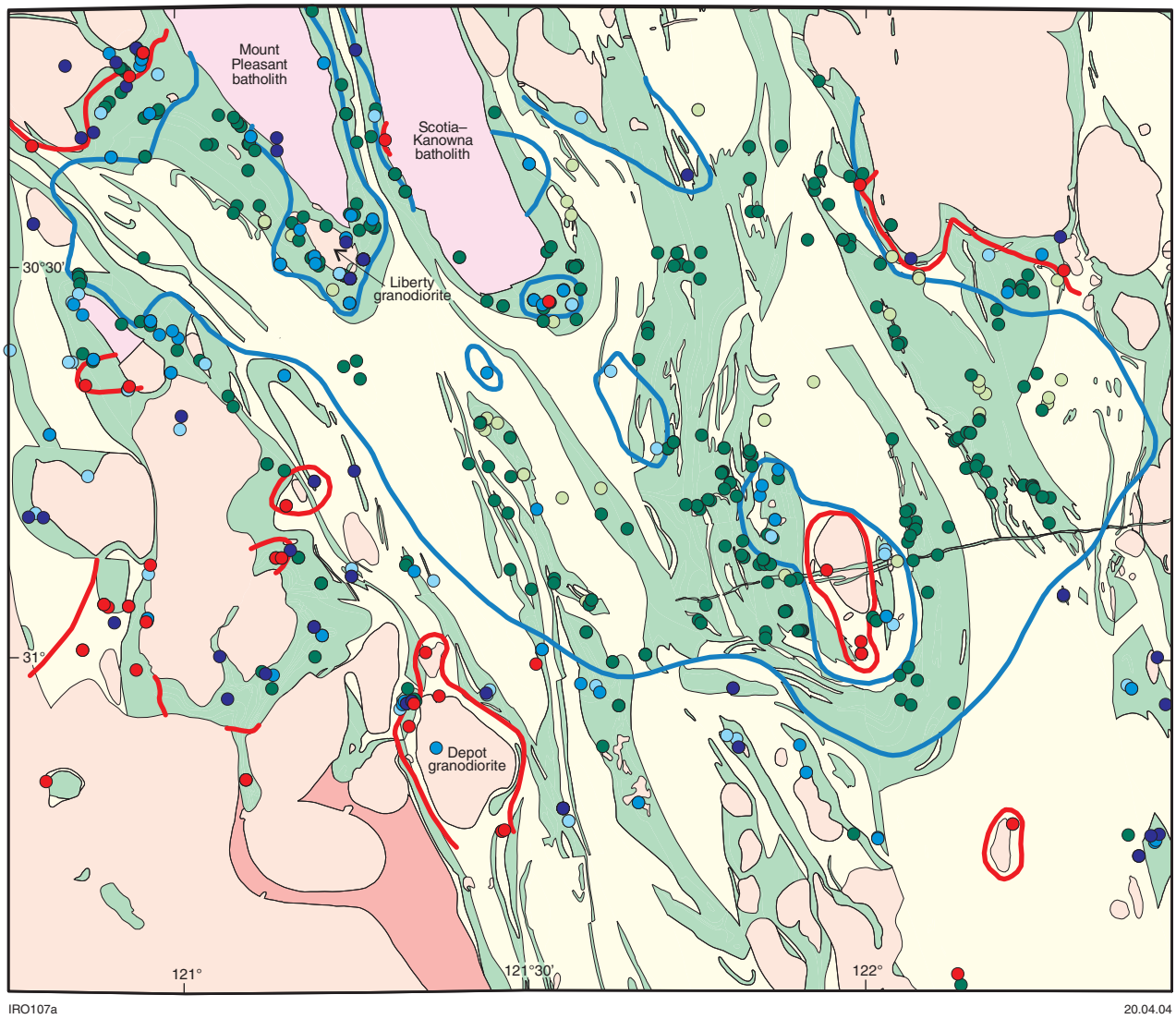

Figure 11. Metamorphic assemblage map for mafic rocks. Sample points are colour coded according to metamorphic zone assemblage. The $B_{(bgamp)}$ zone code represents blue-green amphibole assemblages in which plagioclase type cannot be determined. Isograds are based on the first appearance of blue-green amphibole and green or green-brown hornblende (simplified geology after Vanderhor and Flint, 2001)

a contact-metamorphic rock (pyroxene-hornfels facies) rather than a rock regionally metamorphosed by granulite-facies conditions.

Metamorphic patterns

The metamorphic patterns within the Kalgoorlie region of the Eastern Goldfields Granite–Greenstone Terrane are illustrated in Figures 11 to 14. An interpreted metamorphic-facies map for the region is shown in Figure 15.

The isograds depicted in these figures reflect the progressive mineralogical changes with metamorphic grade summarized in the sections above. They were chosen because they correspond to important facies boundaries (Fig. 7) or changes in metamorphic grade, and because the METPET database provides sufficient

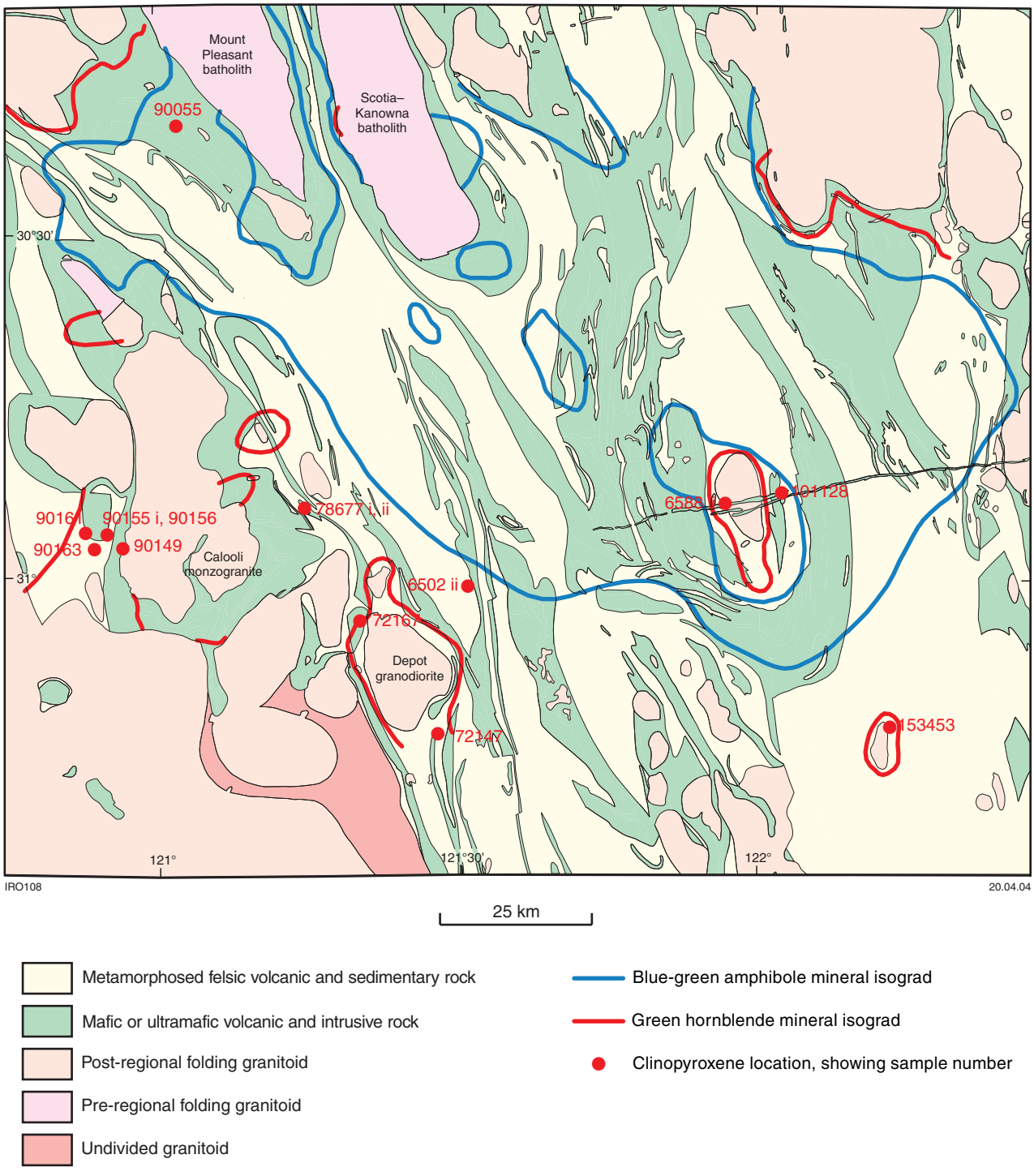

Figure 12. Distribution of diopside in metamorphosed mafic rocks. The mineral isograds are as those shown in Figure 11 (simplified geology after Vanderhor and Flint, 2001)

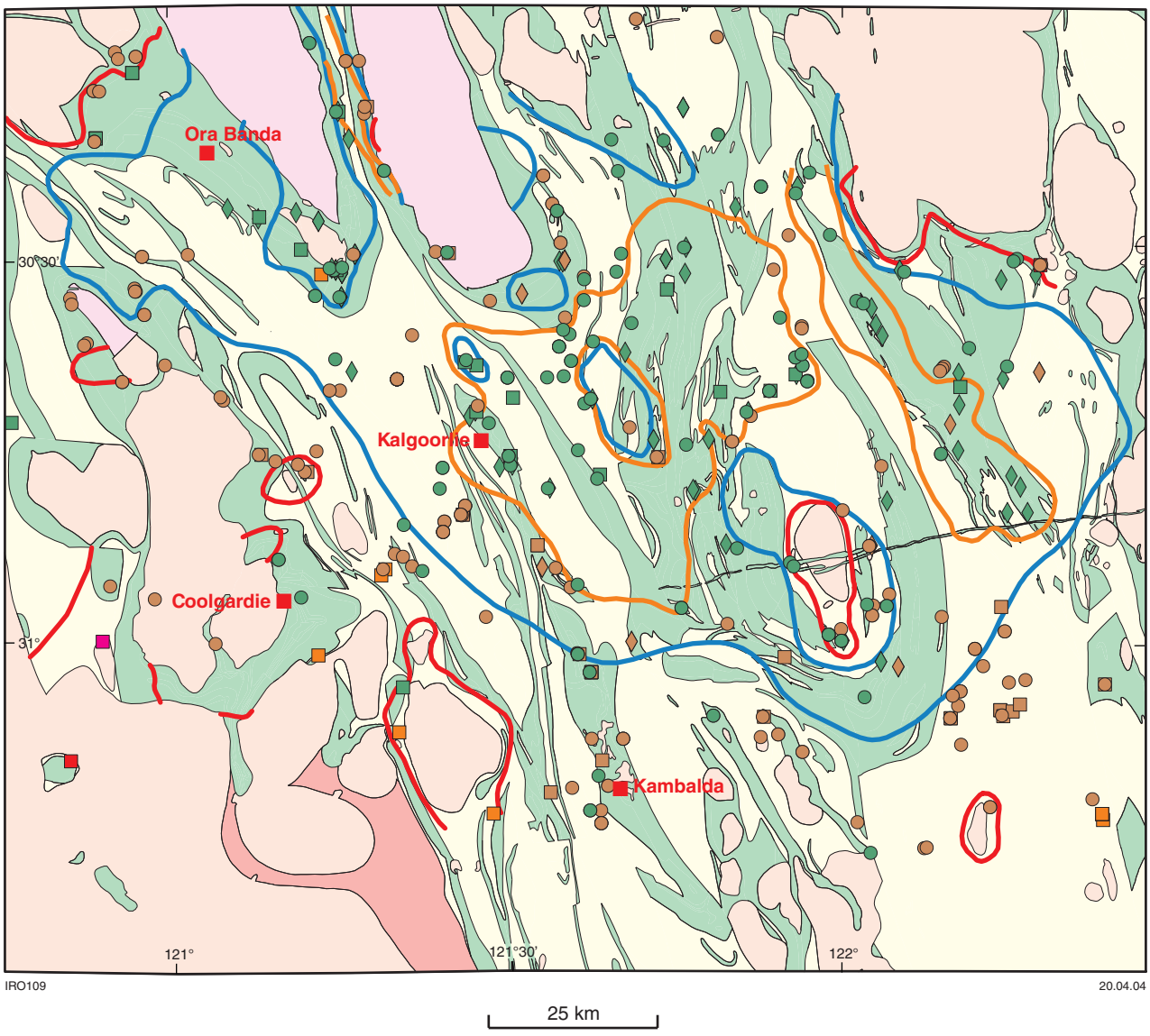

Figure 13. Metamorphic assemblage map for quartzofeldspathic rock types and pelites. The first appearance of biotite in mafic rocks during low-P series metamorphism occurs at nearly the same temperature (or lower) than in quartzofeldspathic and pelitic rock types. Therefore, in areas lacking quartzofeldspathic and pelitic rock types, the 'biotite-in' isograd is constrained by metabasite mineral assemblages (simplified geology after Vanderhor and Flint, 2001)

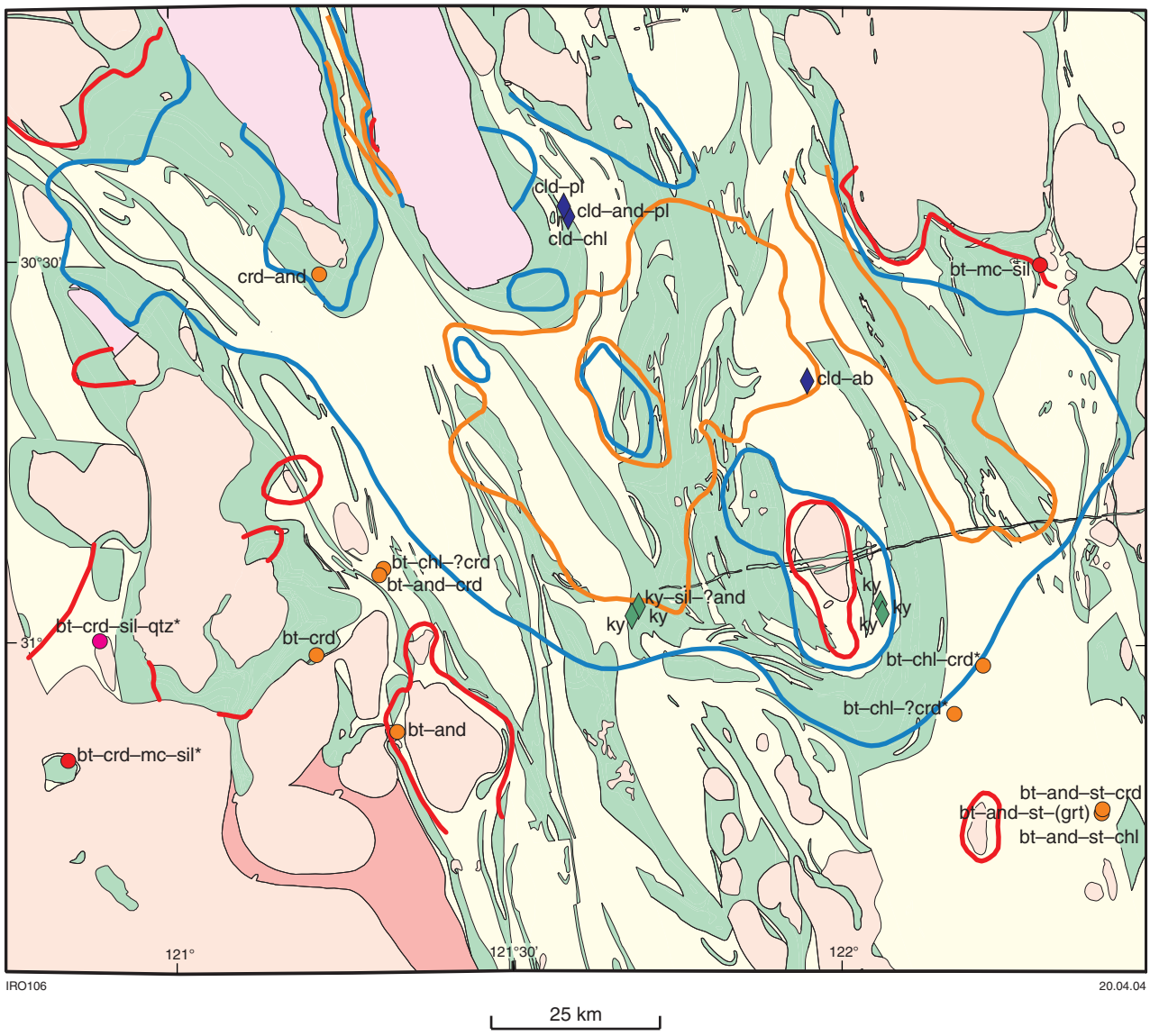

Figure 14. Location of key pelitic and high-alumina assemblages. Note the close proximity of andalusite- and sillimanite-zone pelites to post-regional folding granitoids and to the green hornblende isograd, suggesting that high-grade domains are more restricted than indicated in earlier metamorphic grade maps (simplified geology after Vanderhor and Flint, 2001)

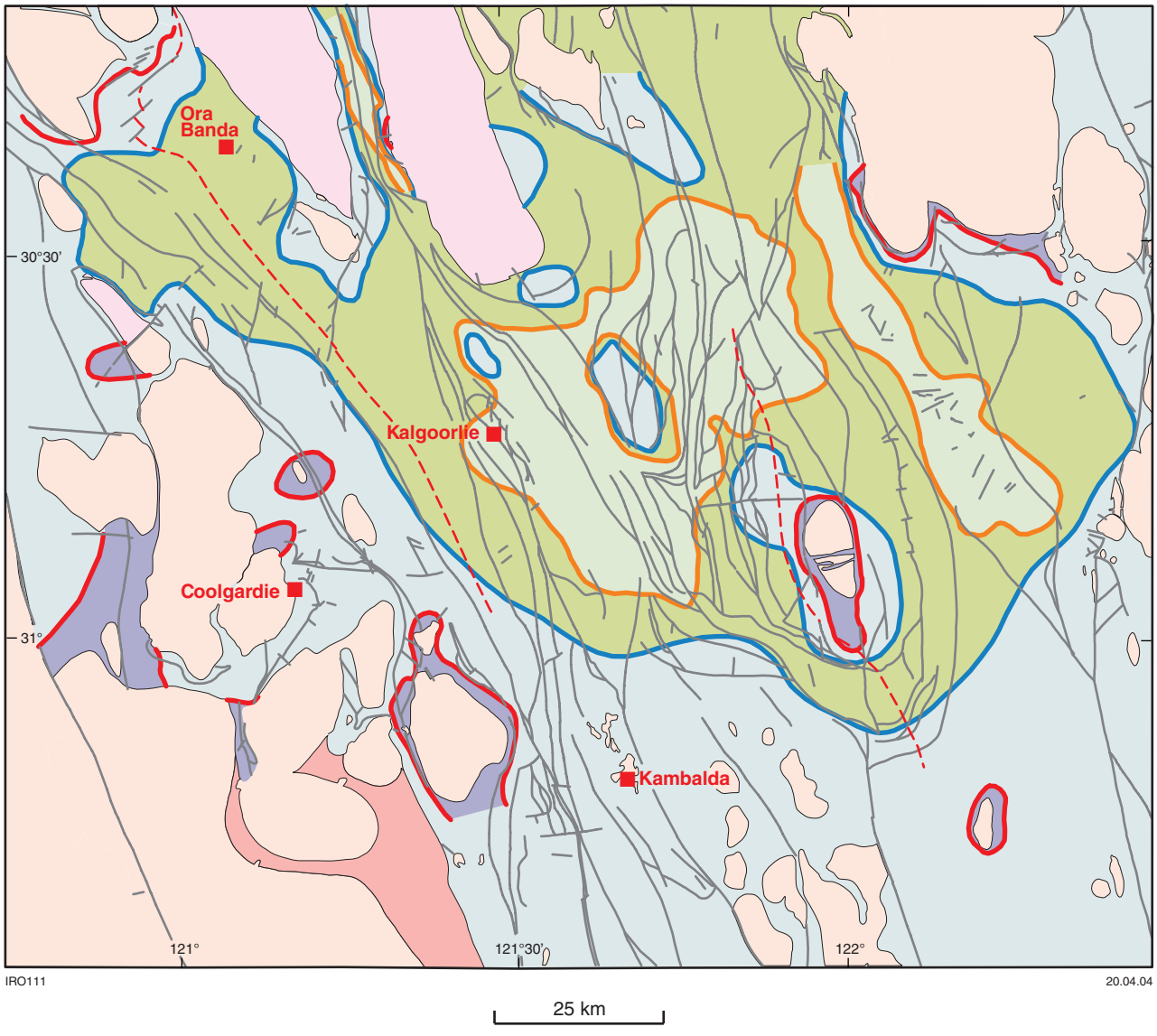

Figure 15. Distribution of metamorphic facies in the Kalgoorlie region (geology after Vanderhor and Flint, 2001)

sample points to reasonably constrain isograd placement. In areas of intermediate to high metamorphic grade, the blue-green-amphibole and green-hornblende isograds derived from metabasite rock assemblages were used to differentiate greenschist-, lower amphibolite-, and upper amphibolite-facies domains. In areas of lower metamorphic grade, regions of greenschist-facies rocks were subdivided into chlorite and biotite subzones based mainly on assemblages in pelitic and quartzofeldspathic rocks. In some areas, the distribution of biotite–muscovite and muscovite–chlorite assemblages in mafic greenschists was also used (see **Mafic rocks**). In regions where isograd placement is poorly constrained by the available data, a tentative placement is given, taking into consideration metamorphic assemblages from other rock types, either from the METPET database or literature (e.g. kyanite–andalusite–chloritoid assemblages in the Steeple Hill area; Swager, 1994).

In many aspects, the revised metamorphic maps agree with previous versions (Binns et al., 1976; Witt, 1993b, Witt et al., 1997; Groenewald et al., 2000; Knight et al., 2000). Common points include the 'concentric' nature of the metamorphic isograds, with higher grades marginal to the granitoids and lower grades located more towards the centre of the greenstone belt (Fig. 15). There are, however, several differences in detail between the current metamorphic maps and those produced by earlier workers. Previous versions of the map portray the western margin of the greenstone belt as a broad zone of high-grade metamorphism that occupies virtually all of the Bullabulling and Coolgardie domains. The METPET dataset is more consistent with a series of much narrower, high-grade aureoles surrounding post-regional folding granitoids and set within a broader region of lower to mid-amphibolite-facies rocks. This conclusion is supported by the following:

- Green hornblende and clinopyroxene in mafic rocks (indicative of upper amphibolite facies) are largely restricted to very narrow zones marginal to intrusive units or in greenstone re-entrants between adjacent plutons (e.g. the Depot granodiorite; Figs 11 and 12).
- Biotite–andalusite-, biotite–sillimanite- and sillimanite–K-feldspar-zone metapelites (upper amphibolite facies) are only located close to granite contacts or to the green-hornblende isograd (Fig. 13).
- Areas previously portrayed as high-grade zones contain lower temperature, blue-green-amphibole assemblages in mafic rocks. These areas include parts of the Bullabulling domain, northwest of the Silt Dam monzogranite, and parts of the Coolgardie domain, south and east of the Bali and Calooli monzogranites (Fig. 11).

Although the sample spacing is still too large to be definitive, the evolving picture for these western greenstone domains is one of wider areas of lower to mid-amphibolite-facies grade interspersed with relatively narrow mid- to upper amphibolite-facies aureoles adjacent to granite margins.

The other main difference between the set of maps in this study (Figs 11–15) and earlier versions is in their portrayal of low-grade metamorphic boundaries within the Kalgoorlie area. Many of the more recent publications (Witt, 1993b; Witt et al., 1997; Groenewald et al., 2000; Knight et al., 2000) only differentiate lower to middle greenschist-facies areas from regions of upper greenschist- to lower amphibolite-facies grade. The corresponding isograd mapped by these workers roughly corresponds to the blue-green amphibole isograd of Figure 11 and is better suited to separating greenschist- from lower amphibolite-facies domains.

Binns et al. (1976) identified two regions of very low metamorphic grade within the Kalgoorlie region, and postulated that these regions also correspond to areas of greatest thicknesses within the greenstone sequence based on gravity data (confirmed by seismic data; Swager, 1997). However, the study failed to specify the facies type, or types (zeolite, prehnite–pumpellyite or lower greenschist facies), that make up the very low grade domains in the Kalgoorlie area. This study did not identify any rocks with zeolite or prehnite–pumpellyite facies assemblages. Biotite–muscovite-bearing versus biotite-absent metasedimentary and quartzofeldspathic rocks (Qf and P groups) were therefore plotted in an attempt to distinguish lower greenschist-facies (chlorite zone) from upper greenschist-facies (biotite zone) areas.

Figure 13 presents the results, with the addition that mafic rock assemblages are used to define the biotite isograd in regions where metasedimentary and quartzofeldspathic rocks are poorly represented. Poorly defined zones of biotite-absent rocks are roughly coincident with the very low grade zones mapped by Binns et al. (1976), along a tight corrodor that coincides with the Boorara Shear Zone between the Mount Pleasant and Scotia–Kanowna batholiths, and in a linear trend along the contact between greenstones and the Penny Dam Conglomerate. The origins of these zones remain uncertain, in part due to the difficulties in differentiating weak carbonate alteration from low-grade regional metamorphism. At least some of the areas reflect zones of weak, post-metamorphic hydrothermal alteration rather than true lower greenschist-facies regional metamorphism (e.g. along the Boorara Shear Zone). The strong linear nature of the easternmost zone of biotite-absent rocks, and its localization along the contact between a thick metaconglomerate unit and greenstones, suggest that it resulted from sea-floor alteration.

Timing of metamorphism with respect to deformation

The relative timing between metamorphism and deformation is complex. Available evidence (Witt, 1991; Swager et al., 1992) indicates that regional metamorphism occurred over an extended time period, from essentially syn-D_2 to late D_3. Evidence for an early, D_1, high-grade metamorphic event associated with the emplacement of pre-regional folding granitoids into the base of the greenstone pile exists in areas to the north and east of the study area (Swager and Nelson, 1997; Witt and Davy, 1997). However, evidence for this event in the Kalgoorlie region has not been recognized, and it is not considered here.

Relationships between metamorphism and D_2 structures are well illustrated within the Kunanalling Syncline area. Here, peak greenschist-facies metamorphic minerals define an S_2, axial-planar schistosity within the metasedimentary rocks (Hunter, 1993). Intrusion of post-regional folding granitoids to the northwest resulted in displacement of the synclinal axis to the east and superimposed an amphibolite-facies metamorphic aureole over the northern, deformed part of the syncline (Fig.11).

Even though metamorphic patterns are often quoted as cutting across terrane boundary faults, facies boundaries are often depicted as being faulted out along the Kunanalling, Zuleika, and Boorara Shear Zones (e.g. Witt, 1993b; Witt et al., 1997; Groenewald et al. 2000; Knight et al., 2000). For example, the Zuleika Shear is commonly shown as separating relatively high grade rocks of the Coolgardie domain from lower grade rocks in the Ora Banda and Kambalda domains for as far south as Widgiemooltha. For the most part, there are insufficient data in key localities to test these relationships. South of the Mungari granite the same blue-green-amphibole assemblages characterize mafic rocks on either side of the Zuleika Shear (Fig. 11), and evidence for a significant discontinuity in metamorphic grade across the fault is lacking. To the north, near the vicinity of the Kundana gold prospect, the Zuleika Shear does appear to separate lower amphibolite-facies from greenschist-facies mafic rocks. However, the position of the blue-green-amphibole isograd in this region is poorly constrained and the small angle between the isograd and the shear zone make interpretation difficult.

In other areas there is clear evidence that the blue-green-amphibole isograd transgresses a number of domain- and terrane-bounding shear zones and other major regional D_3 fault zones at large angles. Examples include the Abatoir, Boulder-Lefroy and Mount Monger Fault zones in the central regions of the study area and the Avoca Fault to the east. In general, regional metamorphism appears to have been initiated during D_2 regional folding and continued until D_3 sinstral faulting was largely completed. Possible offset of the blue-green-amphibole metamorphic isograd along the northern section of the Zuleika Shear Zone indicates that some movement (west side down) along this structure may have occurred after peak metamorphism. Such late movement, if substantiated, may have been in response to post-D_3 extensional collapse of the region, as has been proposed for the Ida Fault to the west (Swager et al., 1997).

Relationship to granitoid plutonism

Opinions vary as to the relative role that granitic magmatism has played in the metamorphism of the Eastern Goldfields greenstone belts (cf. Binns et al., 1976; Bickle and Archibald, 1984; Witt, 1991, 1993b). Witt (1991, 1993b) argued that metamorphic isograds are strongly controlled by proximity to post-regional folding (post-D_2 to syn-D_3) granitoids and that the heat released during crystallization of these magmas strongly influenced the distribution of metamorphic isograds. These effects can be recognized in the Kalgoorlie area at a range of scales (e.g. Fig. 15). For a distance of greater than 70 km along its western side, the blue-green-amphibole isograd roughly parallels the northwesterly trend of a group of post-regional folding granitoids that includes the Depot granodiorite to the south and the Doyle Dam monzogranite to the north. A similar string of northwest-trending plutons in the Parker Hill area, east of Kambalda, deflects the blue-green-amphibole isograd northward by about 15 km.

In the central and northern parts of the study area, metamorphic effects around granitoids tend to be less extensive and more discontinuous. Nevertheless, amphibolite-grade metamorphic aureoles surround many of the smaller plutons and stocks, as well as the larger batholiths to the north. Good examples include the aureoles that surround the Liberty granodiorite and granitic intrusions in the core of the Bulong anticline.

As recognized by Witt (1991, 1993b) and Witt and Davy (1997), the pre-regional folding Mount Pleasant and Scotia–Kanowna batholiths had little influence on metamorphic patterns (Fig. 11). Most amphibolite-grade rocks adjacent to these granitoids appear to be present as 'spot highs' associated with small, satellite plutons peripheral to the main batholiths. Metamorphic rocks around the Liberty granodiorite, just south of the Mount Pleasant batholith, provide a prime example. An analogous 'spot high' directly southeast of the Scotia–Kanowna batholith (Fig. 11) is in a similar structural position to the Liberty granodiorite, and is almost certainly the product of a similar pluton at depth.

Hydrothermal-alteration patterns

Figure 16 shows the distribution of hydrothermal-alteration types associated with mafic-hosted gold mineralization, along with the alteration types for altered metabasite rocks in the METPET database, and interpreted metamorphic isograds. The data for gold occurrences used to construct the figure are given in Appendix 2 and were obtained largely from published sources. Gold-related alteration types plotted in Figure 16 were grouped according to the classification scheme presented by Witt (1993b; table 19) and are also reproduced for this study in Appendix 2. Different alteration types largely reflect differences in the temperature of formation (Mueller and Groves, 1991; Groves et al., 1992; McCuaig and Kerrich, 1994). Note that the alteration codes for METPET samples, which are also plotted, do not correlate exactly with the alteration types used in Appendix 2 because complete alteration-zone sequences could not be determined for the METPET samples. In most cases, it is also impossible to determine whether the alteration assemblages recorded in METPET represent gold-related alteration or one of the other types of carbonate alteration reported from the Eastern Goldfields (e.g. Barley et al., 1990).

Figure 16 encompasses areas studied in detail by Witt (1993b) and Knight et al. (2000), and by and large the

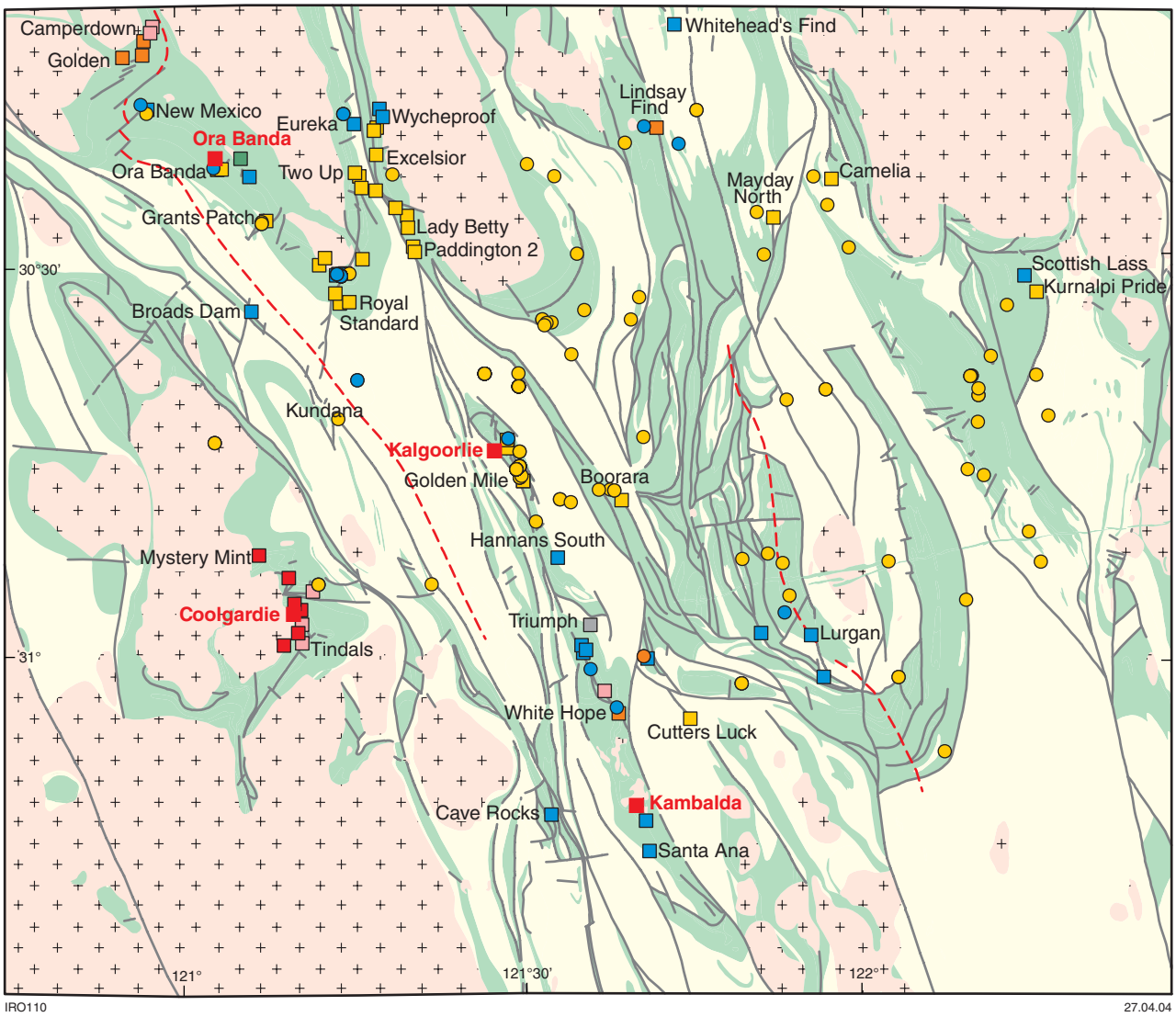

Figure 16. Distribution of hydrothermal-alteration types in mineralized mafic rocks in the Kalgoorlie region. Note that alteration codes for altered metabasite rocks in the METPET database do not correlate exactly with the alteration types associated with mafic-hosted gold mineralization as classified by Witt (1993b — see Appendix 2). This is because complete alteration-zone sequences could not be determined for the METPET samples (simplified geology after Vanderhor and Flint, 2001)

results of this work are consistent with those of these previous studies. Differences are most pronounced in the area southwest of the Mount Pleasant batholith between Mount Pleasant and Siberia, where a number of gold occurrences previously classified as containing low-temperature, sericite–ankerite–chlorite alteration (Witt, 1993b) have here been reclassified as deposits with biotite–chlorite alteration (Type B in Table A2-1). This was justified because all the deposits in question contain biotite as an alteration phase, and because detailed studies at the Golden Kilometre mine indicate that biotite is an integral, although minor, phase in the alteration sequence, at least at that deposit (Gebre-Mariam, 1994). The other deposits in question are relatively close to Golden Kilometre and are in geologically similar settings, so they were all reclassified as deposits with biotite–chlorite alteration. Other differences between this work and earlier studies are due to the inclusion of new gold occurrences (e.g. Broads Dam) and the METPET data.

The revised alteration-distribution map (Fig. 16) still highlights the broad correlation between alteration type and regional metamorphic grade previously documented by Phillips and Groves (1983), Witt (1991, 1993b), and Knight et al. (2000), amongst others. For the most part, each alteration type is restricted to a relatively narrow range of metamorphic grades. Low-temperature, sericite–ankerite–chlorite alteration predominates in chlorite- and biotite-subzone, greenschist-facies domains, whereas intermediate-temperature, biotite–chlorite alteration straddles the boundary between biotite-zone, upper greenschist-facies rocks and lower amphibolite-facies rocks of the blue-green-amphibole zone. High-temperature, hornblende-stable alteration types are present in mafic rocks of either the blue-green-amphibole or green-hornblende metamorphic zones. However, the majority of deposits containing high-temperature alteration are in close proximity to post-regional folding granitoids, and thus likely to have formed in mid- to upper amphibolite-grade host rocks. High-temperature alteration occurrences in the Celebration–Mount Martin area probably indicate that similar intrusions exist at depth (Witt, 1993b).

Like the regional metamorphic patterns, the distribution of gold-related alteration types is thought to reflect proximity to major, post-regional folding granitoids (Witt, 1991, 1993b; Knight et al., 2000). This can be seen in the change from K-feldspar-stable to K-feldspar-absent alteration with increasing distance from the Calooli monzogranite in the high-temperature deposits of the Coolgardie region, and in the transition from high-temperature, hornblende-stable alteration to intermediate-temperature, biotite–chlorite alteration with distance from the Battery monzogranite in the Siberia area (summarized in Fig. 16; see original sources for details).

Witt (1993b) argued against a similar relationship existing between pre-regional folding granitoids of the area and gold mineralization. Based on an interpreted isograd that separated muscovite-dominant from biotite-dominant alteration types and transgressed the Mount Pleasant batholith without being deflected around its contact (Witt, 1993b, fig. 39), he argued that this pre-regional folding granitoid had no effect on alteration isograds because it significantly pre-dated gold mineralization. In actuality, biotite-stable alteration is locally present from south of Golden Kilometer to just south of Siberia, and as far west as the Zuleika Shear Zone (Fig. 16). This puts into question Witt's original alteration isograd in the region southwest of the Mount Pleasant batholith and negates any argument based solely on alteration patterns, but does not necessarily rule out other (e.g. geochronological) evidence for an earlier timing for granite intrusion.

The revised alteration-distribution map presented here may also have significance for the timing between gold mineralization and the string of late-tectonic granitoids that include the Liberty granodiorite and a number of small stocks and plutons extending northward to the Siberia area. Grouped around these small plutons are clusters of gold occurrences that include both sericite–ankerite–chlorite and biotite–chlorite alteration types (Fig. 16). In the case of the Liberty granodiorite, gold occurrences appear to be centred over the southeastern corner of the intrusion, and zone outwards from biotite–chlorite alteration in the Golden Kilometre and Mount Pleasant deposits, to sericite–ankerite–chlorite alteration in the outlying occurrences. It is tempting to speculate that this apparent zonation, and the small biotite–chlorite alteration occurrences associated with the other plutons to the northwest, results from thermal anomalies and gradients associated with the cooling plutons. If so, at least some gold mineralization must be contemporaneous with these late-tectonic granitoids.

Conclusion

The METPET database and its accompanying viewing software (GeoVIEWER.WA) provide a versatile tool, within a spatial context, for the investigation and portrayal of metamorphic-grade variations in the Kalgoorlie region of the Eastern Goldfields. The GIS format allows users to directly compare the placement of metamorphic-facies boundaries or isograds to the data upon which they are based, regardless of scale. Differences in detail between the revised maps presented here and published metamorphic maps (e.g. Binns et al., 1976; Witt et al., 1997; Groenewald et al., 2000), or the user's own maps, can therefore be critically assessed.

Understanding the complex interrelationships between metamorphism, granitic magmatism, and mineralization is an essential prerequisite to understanding the tectonothermal evolution of the Eastern Goldfields and, ultimately, the origin of the hydrothermal systems responsible for gold mineralization. The revised metamorphic maps produced for this study corroborate many of the previous interpretations and go some way towards resolving differences. For example, the METPET data support the presence of a low-grade (lower greenschist facies) central region to the greenstone belt (cf. Binns et al., 1976). The data also highlight the critical role that post-regional folding granitoids had in controlling the distribution of peak metamorphic isograds (cf. Witt, 1993b; Witt and Davy, 1997). At present, it is uncertain whether intrusion of post-regional folding granitoids over

a protracted time span (?c. 2.67 – 2.63 Ga) was, itself, soley responsible for metamorphism or whether the thermal effects of granitiod intrusion were superimposed on an already elevated geothermal gradient (Bickle and Archibald, 1984). Barton and Hanson (1989) stated that magmatic heat advection is sufficient to produce low-pressure metamorphic belts where intrusions form greater than 50% of the upper crust. Low-pressure metamorphic belts can thus develop through the cumulative effect of numerous local, short-lived (less than 1 m.y.) metamorphic events, superimposed onto lower grade regional metamorphic conditions.

By comparison, the metamorphic signatures of the pre-regional folding granitoids of the Mount Pleasant and Scotia–Kanowna batholiths are relatively insignificant and discontinuous. In fact, most of the metamorphic effects generally attributed to these batholiths (e.g. Groenewald et al., 2000) are associated with small satellite intrusions situated along the margins of the pre-folding granitoids. These smaller intrusions have been classified as late-tectonic granitoids by Witt and Davy (1997) and clearly post-date the pre-regional folding intrusions.

The discrepancy between the geochronological evidence for c. 2.63 – 2.60 Ga gold mineralization in greenschist- and lower amphibolite-grade domains on the one hand (Clark et al., 1989; Kent and McDougall, 1995), and field and textural evidence for an essentially syn-metamorphic, synintrusive timing for high-temperature deposits on the other (Witt, 1991, 1993b), has yet to be resolved. The data from METPET and those compiled for known gold occurrences throughout the Kalgoorlie region of the Eastern Goldfields support the findings of Witt (1991, 1993b) and suggest that some post-regional folding granitoids must have provided at least a thermal contribution to some of the lode-gold hydrothermal systems. If this is the case, gold mineralization in the Kalgoorlie area probably took place over a time span of at least 30–35 m.y., rather than within a single 2.63 Ma event (McNaughton et al., 1993).

The general correlation between alteration type and peak metamorphic grade documented here, and elsewhere, indicates that gold mineralization in all metamorphic domains took place during or after peak regional metamorphism but before elevated metamorphic geotherms collapsed back to their pre-metamorphic, steady-state conditions. If so, this implies a metamorphic event of about 30–35 m.y. duration. It is not yet known whether such a scenario is consistent with the tectonothermal setting of the Eastern Goldfields. Other heat sources, in addition to the intrusion of voluminous, post-regional folding granitoids at c. 2.65 – 2.60 Ga, may be required in order to produce such a protracted heating event. One likely source could be heating associated with crustal thinning during post-D_3 extensional collapse (Swager, 1997). In this model, the heat source ultimately responsible for deriving gold-bearing hydrothermal fluids (through metamorphic devolatilization reactions; Phillips and Powell, 1993) and for driving hydrothermal advection would switch from intrusive sources early in the metamorphic history to tectonic thinning in the last stages of metamorphism. Most of the larger gold deposits, situated in lower grade metamorphic areas, are probably associated with the latter event.

Acknowledgements

This study was instigated at the suggestion of Greg Hall of Placer Dome Asia Pacific Limited, and his initial support and the financial support of Placer Dome are acknowledged. Robert Fagan from the Western Australian School of Mines was responsible for many of the earlier thin-section descriptions, and this assistance and his comments on the manuscript are appreciated.

References

AHMAT, A. L., 1986, Metamorphic patterns in the greenstone belts of the Southern Cross Province, Western Australia: Western Australia Geological Survey, Report 19, Professional Papers, p. 1–21.

ARCHIBALD, N., 1998, 3D geology and tectonic synthesis of the Kalgoorlie Terrane, *in* Geodynamics and Gold Exploration in the Yilgarn: Australian Geodynamics Cooperative Research Centre, Perth, W.A., August, 1998, Conference Proceedings, p. 17–22.

BARLEY, M. E., GROVES, D. I., and McNAUGHTON, N. J., 1990, Regional hydrothermal alteration in greenstone belts, *in* Gold deposits of the Archaean Yilgarn Block, Western Australia: Nature, Genesis and Exploration Guides *edited by* S. E. HO, D. I. GROVES, and J. M. BENNETT: The University of Western Australia, Geology Department (Key Centre) and University Extension, Publication 20, p. 55–59.

BARTON, M. D., and HANSON, R. B., 1989, Magmatism and the development of low-pressure metamorphic belts: implications from the western United States and thermal modelling: Geological Society of America Bulletin, v. 101, p. 1051–1065.

BELL, B., GOLEBY, B. R., FOMIN, T., OWEN, A. J., and KORSCH, R. J., 2000, Detailed gravity as an aid for constraining crustal structures interpreted from deep seismic reflection profiling within the Eastern Goldfields, Western Australia: Geological Society of Australia, Abstracts, v. 59, p. 29.

BICKLE, M. J., and ARCHIBALD, N. J., 1984, Chloritoid and staurolite stability: implications for metamorphism in the Archaean Yilgarn Block in Western Australia: Journal of Metamorphic Geology, v. 2, p. 179–203.

BINNS, R. A., GUNTHORPE, R. J., and GROVES, D. I., 1976, Metamorphic patterns and development of greenstone belts in the Eastern Yilgarn Block, Western Australia, *in* The early history of the Earth *edited by* B. F. WINDLEY: New York, John Wiley and Sons, p. 303–313.

BROWN, S. J. A., KRAPEZ, B., BERESFORD, S. W., CASSIDY, K. F., CHAMPION, D. C., BARLEY, M. E., and CAS, R. A. F., 2001, Archaean volcanic and sedimentary environments of the Eastern Goldfields Province, Western Australia — a field guide: Western Australia Geological Survey, Record 2001/13, 66p.

CHAMPION, D. C., 1997, Granitoids in the Eastern Goldfields, in Kalgoorlie '97, Extended abstracts: Australian Geological Survey Organisation, Record 1997/41, p. 71–76.

CHAMPION, D. C., and SHERATON, J. W., 1993, Geochemistry of granitoids in the Leonora–Laverton region, Eastern Goldfields Province, *in* Kalgoorlie '93, Extended Abstracts: Australian Geological Survey Organisation, Record 1993/54, p. 39–46.

CHAMPION, D. C., and SHERATON, J. W., 1997, Geochemistry and Nd isotope systematics of Archaean granites of the Eastern Goldfields, Yilgarn Craton, Australia: implications for crustal growth processes: Precambrian Research, v. 83, p. 109–132.

CLARK, M. E., CARMICHAEL, D. M., HODGSON, C. J., and FU, M., 1989, Wall-rock alteration, Victory Gold Mine, Kambalda, Western Australia: processes and P–T–X_{CO_2} conditions of metasomatism, *in* The geology of gold deposits: the perspective in 1988 *edited by* R.R. KEAYS, W. R. H. RAMSAY, and D. I. GROVES: Economic Geology, Monograph 6, p. 445–459.

DALSTRA, H. J., RIDLEY, J. R., BLOEM, E. J. M., and GROVES, D. I., 1999, Metamorphic evolution of the central Southern Cross Province, Yilgarn Block, Western Australia: Australian Journal of Earth Sciences, v. 46, p. 765–784.

DEER, W. A., HOWIE, R. A., and ZUSSMAN, J., 1966, An introduction to the rock-forming minerals: London, Longman Group Limited, 528p.

DONALDSON, M. J., 1981, Redistribution of ore elements during serpentinization and talc-carbonate alteration of some Archaean dunites, Western Australia: Economic Geology, v. 76, p. 1698–1713.

DONALDSON, M. J., and BROMLEY, G. J., 1981, The Honeymoon Well nickel sulfide deposits, Western Australia: Economic Geology, v. 76, p. 1550–1564.

FAGAN, R. K., 1998, WAGSRK database: Western Australian School of Mines (unpublished).

GEBRE-MARIAM, M., 1994, The nature and genesis of Archaean mesozonal to epizonal gold deposits of the Mt Pleasant area, near Kalgoorlie, Western Australia: University of Western Australia, PhD thesis (unpublished).

GELINAS, L., MELLINGER, M., and TRUDEL, P., 1982, Archean mafic metavolcanics from the Rouyn–Noranda district, Abitibi Greenstone Belt, Quebec — 1. Mobility of the major elements: Canadian Journal of Earth Sciences, v. 19, p. 2258–2275.

GOLEBY, B. R., RATTENBURY, M. S., SWAGER, C. P., DRUMMOND, B. J., WILLIAMS, P. R., SHERATON, J. E., and HEINRICH, C. A., 1993, Archaean crustal structure from seismic reflection profiling, Eastern Goldfields, Western Australia: Australian Geological Survey Organisation, Record 1993/15, 54p.

GRIFFIN, T. J., 1990, Eastern Goldfields Province, *in* Geology and mineral resources of Western Australia: Western Australia Geological Survey, Memoir 3, p. 77–119.

GROENEWALD, P. B., PAINTER, M. G. M., ROBERTS, F. I., McCABE, M., and FOX, A., 2000, East Yilgarn Geoscience Database, 1:100 000 geology Menzies to Norseman — an explanatory note: Western Australia Geological Survey, Report 78, 53p.

GROVES, D. I., BARLEY, M. E., BARNICOAT, A. C., CASSIDY, K. F., FARE, R. J., HAGEMANN, S. G., HO, S. E., HRONSKY, J. M. A., MIKUCKI, E. J., MUELLER, A. G., McNAUGHTON, N. J., PERRING, C. S., RIDLEY, J. R., and VERNCOMBE, J. R., 1992, Subgreenschist- to granulite-hosted Archaean lode-gold deposits of the Yilgarn Craton: a depositional continuum from deep-sourced hydrothermal fluids in crustal-scale plumbing systems: University of Western Australia, Geology Department and University Extension, Publication 22, p. 235–338.

GROVES, D. I., and PHILLIPS, G. N., 1987, The genesis and tectonic controls on Archaean gold deposits of the Western Australian Shield: a metamorphic replacement model: Ore Geology Reviews, v. 2, p. 287–322.

HAMMOND, R. L., and NISBET, B. W., 1992, Towards a structural and tectonic framework for the Norseman-Wiluna greenstone belt, Western Australia, *in* The Archaean: terrains, processes and metallogeny *edited by* J. E. GLOVER and S. E. HO: University of Western Australia, Geology Department and University Extension, Publication no. 22, p. 39-50.

HARTE, B., and HUDSON, N. F. C., 1979, Pelite facies series and the temperature and pressures of Dalradian metamorphism in Eastern Scotland, *in* The Caledonides of the British Isles — Reviewed *edited by* A. L. HARRIS, C. H. HOLLAND, and B. E. LEAKE: Geological Society of London, Special Publication, no. 8, p. 323–337.

HUNTER, W. M., 1991, Boorabbin, W.A. (2nd edition): Western Australia Geological Survey, 1:250 000 Geological Series Explanatory Notes, 46p.

HUNTER, W. M., 1993, Geology of the granite–greenstone terrane of the Kalgoorlie and Yilmia 1:100 000 sheets, Western Australia: Western Australia Geological Survey, Report 35, 80p.

KENT, A. J. R., and McDOUGALL, I., 1995, $^{40}Ar/^{39}Ar$ and U-Pb age constraints on the timing of gold mineralization in the Kalgoorlie gold field, Western Australia: Economic Geology, v. 90, p. 845–859.

KNIGHT, J. T., RIDLEY, J. R., and GROVES, D. I., 2000, The Archaean amphibolite facies Coolgardie goldfields, Yilgarn Craton, Western Australia: nature, controls, and gold field-scale patterns of hydrothermal wall-rock alteration: Economic Geology, v. 95, p. 49–84.

KRAPEZ, B., BROWN, S., and HAND, J., 1997, Stratigraphic signatures of depositional basins in Archaean volcanosedimentary successions of the Eastern Goldfields Province: Australian Geological Survey Organisation, Record 1997/41, p. 33–38.

LEAKE, B. E., 1978, Nomenclature of amphiboles: Mineralogical Magazine, v. 42, p. 533–563.

McCUAIG, T. C., and KERRICH, R., 1994, P–T–t-deformation-fluid characteristics of lode gold deposits: evidence from alteration systematics, *in* Alteration and alteration processes associated with ore-forming systems *edited by* D. R. LENTZ: Geological Association of Canada, Short Course Notes, v. 11, p. 339–379.

McNAUGHTON, N. J., GROVES, D. I., and WITT, W. K., 1993, The source of lead in Archaean lode gold deposits of the Menzies–Kalgoorlie–Kambalda region, Yilgarn Block, Western Australia: Mineralium Deposita, v. 28, p. 495–502.

McQUEEN, K. G., 1981, Volcanic-associated nickel deposits from around the Widgiemooltha Dome, Western Australia: Economic Geology, v. 76, p. 1417–1443.

MATHER, J. D., 1970, The biotite isograd and the lower greenschist facies in the Dalradian rocks of Scotland: Journal of Petrology, v. 88, p. 150–168.

MIYASHIRO, A., 1973, Metamorphism and Metamorphic Belts: London, George Allen and Unwin, 492p.

MUELLER, A. G., and GROVES, D. I., 1991, The classification of Western Australian greenstone-hosted gold deposits according to wallrock-alteration mineral assemblages: Ore Geology Reviews, v. 6, p. 291–331.

NELSON, D. R., 1997, Evolution of the Archaean granite–greenstone terranes of the Eastern Goldfields, Western Australia: SHRIMP U–Pb Zircon constraints: Precambrian Research, v. 83, p. 57–81.

PHILLIPS, G. N., and GROVES, D. I., 1983, The nature of Archaean gold-bearing fluids as deduced from gold deposits of Western Australia: Journal of the Geological Society of Australia, v. 30, p. 25–39.

PHILLIPS, G. N., and POWELL, R., 1993, Link between gold provinces: Economic Geology, v. 88, p. 1084–1098.

PURVIS, A. C., 1984, Metamorphosed altered komatiites at Mt Martin, Western Australia — Archaean weathering products metamorphosed at the alumino-silicate triple point: Australian Journal of Earth Sciences, v. 31, p. 96–106.

SCHMID, R., FETTES, D., HARTE, B., DAVIS, E., DESMONS, J., and SIIVOLA, J., 2002, Towards a unified nomenclature in metamorphic petrology: 1. How to name a Metamorphic Rock (A proposal on behalf of the IUGS Subcommission on the Systematics of Metamorphic Rocks) Web version of 31.07.2002: IUGS Subcommission on the Systematics of Metamorphic Rocks, <http://www.bgs.ac.uk/SCMR/docs/paper 1/pol_010129.pdf>.

SOLOMON, M., and GROVES, D. I., 1994, The Geology and Origin of Australia's Mineral Deposits: Clarendon Press, Oxford, 951p.

SPEAR, F. S., 1993, Metamorphic phase equilibria and pressure–temperature–time paths: Mineralogical Society of America, Monograph, 799p.

SPEAR, F. S., and CHENEY, J. T., 1989, A petrogenetic grid for pelitic schists in the system SiO_2–Al_2O_3–FeO–MgO–K_2O–H_2O: Contributions to Mineralogy and Petrology, v. 101, p. 149–164.

SWAGER, C. P., 1994, Geology of the Kurnalpi 1:100 000 Sheet: Western Australia Geological Survey, Explanatory Notes, 19p.

SWAGER, C. P., 1995, Geology of the greenstone terranes in the Kurnalpi–Edjudina region, southeastern Yilgarn Craton: Western Australia Geological Survey, Report 47, 31p.

SWAGER, C. P., 1997, Tectono-stratigraphy of late Archaean greenstone terranes in the southern Eastern Goldfields, Western Australia: Precambrian Research, v. 83, p. 11–42.

SWAGER, C. P., GOLEBY, B. R., DRUMMOND, B. J., RATTENBURY, M. S., and WILLIAMS, P. R., 1997, Crustal structure of granite–greenstone terranes in the Eastern Goldfields, Yilgarn Craton, as revealed by seismic reflection profiling: Precambrian Research, v. 83, p. 43–56.

SWAGER, C. P., and GRIFFIN, T. J., 1990, Geology of the Archaean Terrane (northern and southern sheets): Western Australia Geological Survey, 1:250 000 Geological Map.

SWAGER, C. P., GRIFFIN, T. J., WITT, W. K., WYCHE, S., AHMAT, A. L., HUNTER, W. M., and McGOLDRICK, P. J., 1990, Geology of the Archaean Kalgoorlie Terrane — an explanatory note: Western Australia Geological Survey, Record 1990/12, 54p.

SWAGER, C. P., GRIFFIN, T. J., WITT, W. K., WYCHE, S., AHMAT, A. L., HUNTER, W. M., and McGOLDRICK, P. J., 1995, Geology of the Archaean Kalgoorlie Terrane — an explanatory note: Western Australia Geological Survey, Report 48, 26p.

SWAGER, C. P., and NELSON, D. R., 1997, Extensional emplacement of a high-grade granite-gneiss complex into low-grade greenstones, Eastern Goldfields, Yilgarn Craton, Western Australia: Precambrian Research, v. 83, p. 203–219.

SWAGER, C. P., WITT, W. K., GRIFFIN, T. J., AHMAT, A. L., HUNTER, W. M., McGOLDRICK, P. J., and WYCHE, S., 1992, Late Archaean granite-greenstones of the Kalgoorlie Terrane, Western Australia, *in* The Archaean: terrains, processes and metallogeny *edited by* J. E. GLOVER and S. E. HO: University of Western Australia, Geology Department and University Extension, Publication no. 22, p. 107–122.

TROMMSDORF, V., and EVANS, B. W., 1977, Antigorite-ophicarbonates: phase relations in a portion of the system CaO–MgO–SiO_2–H_2O–CO_2: Contributions to Mineralogy and Petrology, v. 60, p. 39–56.

VANDERHOR, F., and FLINT, R. B. (compilers), 2001, Interpreted bedrock geology of Western Australia, preliminary edition (1:500 000 scale): Western Australia Geological Survey.

WITT, W. K., 1991, Regional metamorphic controls on alteration associated with gold mineralization in the Eastern Goldfields Province, Western Australia: implications for the timing and origin of Archaean lode-gold deposits: Geology, v. 19, p. 982–985.

WITT, W. K., 1993a, Lithological and structural controls on gold mineralization in the Archaean Menzies–Kambalda area, Western Australia: Australian Journal of Earth Sciences, v. 40, p. 65–86.

WITT, W. K., 1993b, Gold mineralization in the Menzies–Kambalda region, Eastern Goldfields, Western Australia: Western Australia Geological Survey, Report 39, 165p.

WITT, W. K., 1994, Geology of the Melita 1:100 000 sheet: Western Australia Geological Survey, 1:100 000 Geological Series Explanatory Notes, 63p.

WITT, W. K., and DAVY, R., 1997, Geology and geochemistry of granitoid rocks in the Southwest Eastern Goldfields Province: Geological Survey of Western Australia, Report 49, 137p.

WITT, W. K., KNIGHT, J. T., and MIKUCKI, E. J., 1997, A synmetamorphic lateral fluid flow model for gold mineralization in the Archaean southern Kalgoorlie and Norseman Terranes, Western Australia: Economic Geology, v. 92, p. 407–437.

WITT, W. K., and SWAGER, C. P., 1989, Structural setting and geochemistry of Archaean I-type granites in the Bardoc–Coolgardie area of the Norseman–Wiluna Belt, Western Australia: Precambrian Research, v. 41, p. 323–351.

WYCHE, S., 1998, Kalgoorlie, W.A. (2nd edition): Western Australia Geological Survey, 1:250 000 Geological Series Explanatory Notes, 31p.

YARDLEY, B. W. D., 1989, An Introduction to Metamorphic Petrology: Longman Group Limited, Essex, 248p.

Appendix 1

Description of digital datasets

The CD-ROM that accompanies this Record contains the following datasets.

Geology

Information on the geology has been extracted from the State 1:500 000 geology dataset, with the granitoid rocks classified according to the scheme proposed by Witt and Davy (1997), and the major tectono-stratigraphic domains after Groenewald et al. (2000). The separate layers or polygon themes supplied are:

- interpreted bedrock geology
- major tectono-stratigraphic domains
- major faults and shear zones
- granitoid-rock classification

Sample points

The METPET database is based on petrographic descriptions of about 2000 thin sections from the collection of the Geological Survey of Western Australia (GSWA). About 75% of descriptions were carried out by Edward Mikucki of E. & J. Mikucki Geological Consultants, and the majority of the remainder by Robert Fagan of the Western Australian School of Mines (Fagan, 1998). Some descriptions by Walter Witt (Witt, W. K., 1997, written comm.) are also included. Descriptions by all petrographers have been combined and presented in the METPET database. Locality information (MGA coordinates) for the thin sections described is from the GSWA WAROX database.

Mineral assemblages

The metamorphic mineral assemblages are displayed digitally on separate layers or polygon themes. They include:

- mineral assemblages in mafic rocks
- mineral assemblages in sedimentary and felsic volcanic rocks
- mineral assemblages in ultramafic rocks
- mineral assemblages for wallrock alteration of mafic host rocks

In addition, there are layers that show:

- the locality of mafic rocks with metamorphic clinopyroxene
- the locality of key pelitic and high-alumina assemblages
- blue-green-amphibole and green-hornblende isograds for mafic rock samples
- biotite isograd for metamorphosed sedimentary and felsic volcanic rocks
- metamorphic isograds based on wallrock alteration of mafic host rocks

References

FAGAN, R. K., 1998, WAGSRK database: Western Australian School of Mines (unpublished).

GROENEWALD, P. B., PAINTER, M. G. M., ROBERTS, F. I., McCABE, M., and FOX, A., 2000, East Yilgarn Geoscience Database, 1:100 000 geology Menzies to Norseman — an explanatory note: Western Australia Geological Survey, Report 78, 53p.

WITT, W. K., and DAVY, R., 1997, Geology and geochemistry of granitoid rocks in the Southwest Eastern Goldfields Province: Geological Survey of Western Australia, Report 49, 137p.

Appendix 2

Wallrock-alteration mineral assemblages for gold deposits in the Kalgoorlie region

Different hydrothermal-alteration types largely reflect differences in the temperature of formation (Mueller and Groves, 1991; Groves et al., 1992; McCuaig and Kerrich, 1994). Table A2-1 summarizes alteration-zoning patterns and assemblages in Witt's (1993) classification scheme for hydrothermal-alteration types.

Table A2-2 is a compilation of observed alteration assemblages and zoning sequences from known gold-related mineral occurrences within the Kalgoorlie region of the Eastern Goldfields. Note that for deposits with mafic host rocks, there are differences between the observed alteration assemblages and those summarized in Table A2-1. This is because the complete alteration-zone sequences could not be determined, and the alteration assemblages recorded in published sources may not specifically represent gold-related alteration.

Table A2-1. Metasomatic and metamorphic assemblages associated with gold-related mineralization in mafic rocks

Hydrothermal alteration type	*Inner alteration zone*	*Outer alteration zone*	*Metamorphic assemblage*
A (300ºC)	**muscovite** **ankerite** **siderite** pyrite pyrrhotite arsenopyrite	**chlorite** **calcite or ankerite** **albite** epidote ilmenite pyrrhotite	**actinolite** **albite** **ilmenite(–epidote)**
B (400ºC)	**quartz** **ankerite** **albite** **muscovite** rutile pyrite	**biotite** **chlorite** **calcite** titanite epidote pyrrhotite pyrite	**actinolite or hornblende** **albite or calcic plagioclase** **ilmenite(–epidote)**
C (500ºC)	**quartz** **biotite** **calcic plagioclase** calcite titanite pyrrhotite pyrite arsenopyrite	**biotite** **hornblende** **calcic plagioclase** calcite garnet ilmenite pyrrhotite pyrite	**hornblende** **calcic plagioclase** **ilmenite**
D (600ºC)	**microcline** **diopside** **garnet** calcic plagioclase calcite pyrrhotite pyrite arsenopyrite	**hornblende** **calcic plagioclase** **biotite** calcite titanite pyrrhotite	**hornblende** **calcic plagioclase** **ilmenite**

SOURCE: Witt (1993, table 19)

NOTES: Minerals in bold represent the dominant minerals in each alteration zone.
Minerals in normal font generally form <10% of the alteration assemblage.
Estimated temperatures of formation are from Witt (1993) and are estimates only.

Table A2-2. Alteration assemblages and zoning sequences from gold deposits in the Kalgoorlie region

Deposit	*MGA coordinates*		*Host rock*	*Alteration type (mafic hosts)*	*Outer alteration zone*	*Intermediate alteration zone*	*Inner alteration zone*	*Reference*
	Easting	*Northing*						
Barbara–Surprise	332672	6573444	metakomatiite	–	tremolite; chlorite; talc; biotite; calcite; pyrrhotite	tremolite; chlorite; talc; biotite; calcite; pyrrhotite	biotite; hornblende; chlorite; plagioclase; talc; quartz	Knight et al. (2000)
Bayleys Reward	328250	6576206	metakomatiite	–	hornblende; tremolite; chlorite; biotite; talc; calcite; pyrrhotite	hornblende; tremolite; chlorite; biotite; talc; calcite; pyrrhotite; arsenopyrite	hornblende; plagioclase; biotite; calcite; chlorite; talc; quartz; titanite	Knight et al. (2000)
Binduli–Centurion	347340	6587148	metasedimentary rocks and porphyry	–	quartz; sericite; pyrite; carbonate; biotite; magnetite; pyrite		quartz; sericite; pyrite; carbonate; pyrite; chalco-pyrite; galena; sphalerite	Ivey et al. (1998)
Black Flag	330456	6619638	low-Mg metabasalt; porphyry	A			quartz; sericite; carbonate; pyrite; fluorite; Fe-poor sphalerite; galena; chalcopyrite	Witt (1993)
Bonnie Doon	302878	6652983	low-Mg metabasalt	B–C(?)	quartz; biotite; carbonate; pyrrhotite	quartz; carbonate; biotite; pyrrhotite	biotite; plagioclase; carbonate; pyrite	Witt (1993)
Bonnievale	324532	6585755	tonalitic granite	–	quartz; K-feldspar; plagioclase; biotite; magnetite; ilmenite	quartz; plagioclase; K-feldspar; biotite; hornblende; magnetite; ilmenite; pyrrhotite	hornblende; plagioclase; biotite; calcite; epidote; quartz; clinozoisite	Knight et al. (2000)
Boorara	370377	6590731	metagabbro–metadolerite; high-Mg or komatiitic metabasalt	A			quartz; carbonate; sericite; pyrite; arsenopyrite	Witt (1993)
Brilliant	326455	6572359	metakomatiite	–	tremolite; chlorite; talc; calcite; biotite; pyrrhotite	tremolite; chlorite; talc; calcite; biotite; pyrrhotite	tremolite; chlorite; talc; calcite; biotite; pyrrhotite	Knight et al. (2000)
Brilliant	326455	6572359	metagabbro–metadolerite	C			hornblende; plagioclase; calcite; quartz; garnet; biotite	Knight et al. (2000)
Broads Dam	318696	6616767	metagabbro–metadolerite	B			quartz; biotite; sericite; chlorite; carbonate; arseno-pyrite; pyrite; pyrrhotite	Glasson et al. (1998)
Burbanks	323988	6569355	high-Mg or komatiitic metabasalt; metagabbro–metadolerite	D	hornblende; plagioclase; biotite; ilmenite; pyrrhotite	hornblende; plagioclase; garnet; biotite; pyrite; ilmenite	biotite; quartz; calcite; hornblende; K-feldspar; garnet	Knight et al. (2000)
Camelia	398967	6636705	metagabbro–metadolerite	A	chlorite; carbonate		quartz; plagioclase; chlorite; sericite; carbonate	Roberts et al. (in prep.)
Camperdown	304218	6657051	low-Mg metabasalt	C	biotite; hornblende; calcic plagioclase; calcite; garnet; ilmenite; pyrrhotite; pyrite		quartz; biotite; calcic plagioclase; calcite; sphene; pyrrhotite; pyrite; arsenopyrite	Witt (1993)
Cave Rocks	361246	6545863	metagabbro–metadolerite	B	chlorite; dolomite		biotite; albite; quartz; pyrrhotite	Watchorn (1998)
Celebration	365347	6568918	porphyry; high-Mg or komatiitic metabasalt	B	chlorite; plagioclase; carbonate; quartz; biotite		biotite; plagioclase; pyrite; carbonate; chlorite; quartz; chalcopyrite; rutile	Witt (1993)
Central Zone	389439	6601311	crystal-lithic tuff	–	chlorite; carbonate; hematite		ankerite; sericite; pyrite;	Roberts et al. (in prep.)
Cock Eyed Bob	421422	6560185	iron-rich metasedimentary rocks	–	magnetite; cummingtonite; hornblende; actinolite; biotite; pyrrhotite; arsenopyrite; chlorite; carbonate		pyrrhotite; arsenopyrite; magnetite; cummingtonite; hornblende; actinolite; biotite; chlorite; carbonate	Newton et al. (1998)

Table A2-2 (continued)

Deposit	*MGA coordinates*		*Host rock*	*Alteration type (mafic hosts)*	*Outer alteration zone*	*Intermediate alteration zone*	*Inner alteration zone*	*Reference*
	Easting	*Northing*						
Craze	424566	6565441	iron-rich metasedimentary rocks	–	magnetite; cummingtonite; hornblende; actinolite; biotite; chlorite; carbonate		pyrrhotite; arsenopyrite; magnetite; cummingtonite; hornblende; actinolite; biotite; chlorite; carbonate	Newton et al. (1998)
Cutters Luck	380207	6559765	amphibolite; undifferentiated mafic rock	A	chlorite; carbonate		quartz; sericite; pyrite	Witt (1993)
Daisy–Milano	397177	6568536	felsic volcaniclastic rock	–	quartz; feldspar; carbonate; muscovite; chlorite; rutile; pyrite		quartz; feldspar; muscovite; rutile; pyrite; tourmaline	Roberts et al. (in prep.)
Ellen Pearce	336025	6645924	low-Mg metabasalt	B	chlorite; carbonate; pyrrhotite	biotite; chlorite; pyrite	biotite; carbonate; pyrite	Witt (1993)
Enterprise	316837	6638512	high-Mg or komatiitic metabasalt	A–B?			sericite; ?biotite; iron sulfide or ?iron carbonate	Witt (1993)
Eureka	332498	6643700	low-Mg metabasalt	B			chlorite; quartz; ankerite; biotite; pyrrhotite	Witt (1993); Ransted (1990)
Excelsior	335670	6643246	high-Mg or komatiitic metabasalt	A			fuchsite; dolomite; ankerite; pyrite	Witt (1993); Bottomer and Robinson (1990)
Flagstaff	325950	6571142	metabasalt and black metashale	D	hornblende; biotite; plagioclase; ilmenite	hornblende; plagioclase; calcite; garnet; chlorite; pyrrhotite; ilmenite	hornblende; chlorite; garnet; calcite; cordierite; plagioclase; K-feldspar	Knight et al. (2000)
Gibraltar	305387	6563182	felsic gneiss (dacitic tuff protolith)	–			garnet; biotite; ferrihastingsite; cummingtonite; tourmaline	Pyke (1990)
Gimlet South (Townsite camp)	313607	6636883	iron-rich low-Mg metabasalt commonly with small to large plagioclase phenocrysts	A	chlorite; calcite; epidote; ilmenite; leucoxene; pyrrhotite		sericite; calcite; ankerite; quartz; titanite; leucoxene; pyrite; arsenopyrite; chlorite; tourmaline	Witt (1993)
Gimlet South (underground)	313606	6636884	low-Mg metabasalt	A	chlorite; calcite; epidote; ilmenite; leucoxene; pyrrhotite		sericite; calcite; ankerite; quartz; titanite; leucoxene; pyrite; arsenopyrite; chlorite; tourmaline	Witt (1993)
Golden Kilometre	330655	6622349	metagabbro–metadolerite	B	chlorite; calcite; ankerite; albite; epidote; ilmenite; pyrrhotite		muscovite; ankerite; siderite; pyrite; pyrrhotite; arsenopyrite	Witt (1993)
Golden	300129	6652581	high-Mg or komatiitic metabasalt	B–C?	biotite; quartz;		quartz; plagioclase; biotite;	Witt (1993)
Golden Arrow	340101	6630747	undifferentiated metabasalt	A	chlorite; carbonate		quartz; sericite; pyrite	Witt (1993)
Golden Buckle	333982	6624504	metagabbro–metadolerite	A	chlorite; carbonate		quartz; sericite; pyrite	Witt (1993)
Golden Hope	368358	6563567	metagabbro–metadolerite	C	quartz; biotite; calcite; ilmenite; hornblende		quartz; calcic plagioclase; calcite; biotite; pyrite; chalcopyrite; rutile; magnetite	Witt (1993)
Golden Mile	356738	6593287	low-Mg metabasalt	A	chlorite; calcite; ankerite; albite; quartz; epidote; ilmenite; pyrrhotite		muscovite; chlorite; ankerite; siderite; pyrite; pyrrhotite	Witt (1993)
Golden Mile	356738	6593287	metagabbro–metadolerite	A	chlorite; calcite; ankerite; albite; quartz; epidote; ilmenite; pyrrhotite		muscovite; chlorite; ankerite; quartz; siderite; pyrite; pyrrhotite	Witt (1993)

Table A2-2 (continued)

Deposit	*MGA coordinates*		*Host rock*	*Alteration type (mafic hosts)*	*Outer alteration zone*	*Intermediate alteration zone*	*Inner alteration zone*	*Reference*
	Easting	*Northing*						
Gordon–Sirdar	365050	6630470	polymictic metaconglomerate	–			carbonate; pyrite; sericite; chlorite	Roberts et al. (in prep.)
Gordon–Sirdar	365050	6630470	aphyric felsic volcaniclastic rock	–			quartz; chlorite; pyrite; sericite; andalusite; chloritoid	Roberts et al. (in prep.)
Grants Patch	320534	6629701	low-Mg metabasalt	A	chlorite; calcite; ankerite; albite; epidote; ilmenite; pyrrhotite		muscovite; ankerite; siderite; pyrite; pyrrhotite	Witt (1993)
Hampton–Boulder	366677	6566503	porphyry	–	sericite; carbonated feldspar		arsenopyrite sericite; quartz; pyrite	Witt (1993)
Hannans South	361643	6582422	high-Mg or komatiitic metabasalt	B	sericite; carbonate		sericite; carbonate; chlorite; biotite; pyrite; arsenopyrite	Witt (1993); Schiller and Ivey (1990)
Hoffmann	389790	6571245	metakomatiite	–	talc; carbonate; chlorite; muscovite		talc; carbonate; chlorite; muscovite	Roberts et al. (in prep.)
Hunt	374293	6545189	low-Mg metabasalt	B	chlorite; biotite; ankerite; calcite		ankerite; biotite; albite; pyrite	Watchorn (1998)
Intrepide	376434	6541649	porphyry	–	chlorite		pyrite; albite; biotite	Watchorn (1998)
Jubilee – New Hampton	366924	6565892	porphyry	–			biotite; chlorite; feldspar; andalusite; amphibole; carbonate; pyrite	Copeland (1998)
Kanowna Belle	363410	6612540	porphyry and felsic volcanic rocks	–	sericite; carbonate; chlorite; hematite	sericite; ankerite; pyrite	pyrite; albite; quartz	Taylor (1984); Beckett et al. (1998)
King Edward	328011	6623553	metagabbro–metadolerite	A			chlorite; calcite; pyrrhotite	Witt (1993)
Kings Cross	326259	6574448	high-Mg or komatiitic metabasalt	D	hornblende; plagioclase; biotite; ilmenite; pyrrhotite	hornblende; plagioclase; biotite; quartz; calcite; ilmenite; pyrrhotite; arsenopyrite	hornblende; plagioclase; biotite; calcite; K-feldspar; quartz; epidote; titanite	Knight et al. (2000)
Kundana	330551	6601145	felsic volcanic and metasedimentary rocks	–			quartz; sericite; biotite; tourmaline; pyrite; pyrrhotite; arsenopyrite	Witt (1993)
Kurnalpi Pride	427577	6620909	low-Mg metabasalt	A	plagioclase; chlorite; carbonate; quartz; epidote; leucoxene; pyrrhotite; pyrite		albite; ankerite; quartz; muscovite; leucoxene; rutile; pyrite	Roberts et al. (in prep.)
Lady Betty	340241	6629073	amphibolite; undifferentiated mafic rock	A	chlorite; carbonate		sericite; pyrite; ?quartz	Witt (1993)
Lady Bountiful	328780	6624570	metagabbro–metadolerite	A			chlorite; carbonate; pyrrhotite; sericite; pyrite	Witt (1993)
Lady Bountiful	328015	6624094	granitoid	–	potassium feldspar; sericite; albite; pyrite		sericite; quartz; chlorite; ilmenite; leucoxene; pyrite	Witt (1993); Bartsch (1990)
Lady Evelyn	318093	6635966	metagabbro–metadolerite	B			chlorite; carbonate; biotite; pyrite; chalcopyrite	Witt (1993)
Lady Loch	327228	6571032	metakomatiite	–	hornblende; tremolite; talc; chlorite; biotite; pyrrhotite	hornblende; tremolite; talc; chlorite; biotite; pyrrhotite; arsenopyrite	hornblende; tremolite; talc; chlorite; biotite; K-feldspar;	Knight et al. (2000)
Lanarkshire	365067	6570023	high-Mg or komatiitic metabasalt	B	biotite; pyrite; pyrrhotite; carbonate; hematite		pyrrhotite; arsenopyrite; quartz; carbonate; pyrite; ?albite	Witt (1993)

Table A2-2 (continued)

Deposit	*MGA coordinates*		*Host rock*	*Alteration type (mafic hosts)*	*Outer alteration zone*	*Intermediate alteration zone*	*Inner alteration zone*	*Reference*
	Easting	*Northing*						
Lindsays Find	374582	6643764	undifferentiated metabasalt	B–C?			plagioclase; carbonate; quartz; chlorite; biotite; pyrite	Roberts et al. (in prep.)
Lindsays Find	374582	6643764	feldspar-quartz porphyry	–			plagioclase; quartz; sericite; carbonate; pyrite; biotite; chlorite; rutile	Roberts et al. (in prep.)
Lindsays	325342	6575297	high-Mg or komatiitic metabasalt	D	hornblende; plagioclase; biotite; ilmenite; pyrrhotite	hornblende; plagioclase; biotite; quartz; calcite; ilmenite; pyrrhotite; arsenopyrite	hornblende; plagioclase; biotite; calcite K-feldspar; quartz; epidote; titanite	Knight et al. (2000)
Lurgan	396783	6571806	mafic rocks (metadolerite and metabasalt)	B			chlorite; biotite; carbonate; quartz; pyrite; pyrrhotite	Roberts et al. (in prep.)
Majestic	397751	6579290	leucocratic feldspar; quartz; amphibole porphyry; mesocratic plagioclase porphyry	–	albite; muscovite; quartz; chlorite; biotite; pyrite; titanite		albite; chlorite; biotite; quartz; pyrite; titanite; rutile	Roberts et al. (in prep.)
Maxwell	423588	6561155	metasedimentary rocks	–	magnetite; cummingtonite; hornblende; actinolite; biotite; chlorite; carbonate		pyrrhotite; arsenopyrite; magnetite; cummingtonite; hornblende; actinolite; biotite; chlorite; carbonate	Newton et al. (1998)
Mayday North	390973	6631161	undifferentiated metabasalt; meta-andesite	A	chlorite; sericite; epidote; albite; leucoxene; pyrite		carbonate; albite; apatite; pyrite; arsenopyrite	Roberts et al. (in prep.)
Mirror Magic	398556	6565902	andesitic metavolcaniclastic rock	B			carbonate; chlorite; biotite; pyrrhotite; pyrite	Roberts et al. (in prep.)
Mirror Magic	398556	6565902	metadacite	–			carbonate; sericite; biotite; pyrite; pyrrhotite; arsenopyrite	Roberts et al. (in prep.)
Missouri	303027	6654994	low-Mg metabasalt	B–C?	quartz; plagioclase; chlorite; biotite; carbonate; pyrite		quartz; plagioclase; biotite; carbonate; pyrite	Witt (1993)
Mount Charlotte	354527	6597911	metagabbro–metadolerite	A	chlorite; albite; magnetite; calcite		quartz; sericite; albite; ankerite; leucoxene; pyrite; pyrrhotite	Clout et al. (1990)
Mount Martin	374239	6568227	metakomatiite	–			quartz; carbonate; albite; pyrrhotite; magnetite	Witt (1993)
Mount Martin	374239	6568227	mafic rocks (dolerite and metabasalt)	B			chlorite; biotite; quartz; carbonate; albite; pyrrhotite; ilmenite	Witt (1993)
Mount Percy	354399	6599105	high-Mg or komatiitic metabasalt	A			quartz; carbonate; sericite; fuchsite; pyrite	Witt (1993)
Mount Percy	354399	6599105	metagabbro–metadolerite	A			talc; carbonate; chlorite	Witt (1993)
Mount Percy	354399	6599105	metakomatiite	–			talc; carbonate	Witt (1993)
Mount Percy	354399	6599105	porphyry	–			carbonate; sericite; pyrite	Witt (1993)
Mount Pleasant (Southern Shoot)	330364	6622161	metagabbro–metadolerite	B	chlorite; carbonate; biotite; pyrrhotite		sericite; carbonate; albite; pyrrhotite; pyrite; ilmenite	Witt (1993)
Mystery Mint	320344	6582083	metagabbro–metadolerite	D	hornblende; plagioclase; quartz; ilmenite	hornblende; plagioclase; quartz; calcite; garnet; pyrite; ilmenite	hornblende; quartz; albite; calcite; K-feldspar; garnet; biotite; chlorite	Knight et al. (2000)
Nerrin Nerrin	335670	6639366	metagabbro–metadolerite	A	chlorite; carbonate		sericite; pyrite	Witt (1993)

Table A2-2 (continued)

Deposit	*MGA coordinates*		*Host rock*	*Alteration type (mafic hosts)*	*Outer alteration zone*	*Intermediate alteration zone*	*Inner alteration zone*	*Reference*
	Easting	*Northing*						
New Mexico	303735	6645274	high-Mg or komatiitic metabasalt	B	biotite; chlorite; calcite; sphene; epidote; pyrrhotite; pyrite		quartz; ankerite; albite; muscovite; rutile; pyrite	Witt (1993)
Ora Banda	314219	6636926	low-Mg metabasalt	A	chlorite; muscovite; calcite; ankerite; albite; epidote; ilmenite; pyrrhotite		muscovite; chlorite; ankerite; siderite; calcite; arsenopyrite; pyrite	Witt (1993); Harrison et al. (1990)
Paddington 1	340994	6626357	metagabbro–metadolerite	A	chlorite; albite; calcite	dolomite; ankerite; sericite; arsenopyrite; pyrite	sericite; ankerite; quartz; arsenopyrite; pyrite; fuchsite	Witt (1993); Hancock et al. (1990)
Paddington 2	341218	6625653	metagabbro–metadolerite	A	chlorite; albite; calcite	dolomite; ankerite; sericite; arsenopyrite; pyrite	sericite; ankerite; quartz; arsenopyrite; pyrite; fuchsite	Witt (1993); Hancock et al. (1990)
Patricia Jean	324512	6578947	metagabbro–metadolerite	D	hornblende; plagioclase; biotite; quartz; ilmenite; pyrrhotite	hornblende; quartz; plagioclase; calcite; garnet; pyrrhotite; ilmenite	hornblende; quartz; plagioclase; calcite; K-feldspar; garnet; pyrrhotite	Knight et al. (2000)
Pernatty	365712	6569354	metagabbro–metadolerite	B	chlorite; biotite; carbonate		biotite; quartz; pyrite	Witt (1993)
Queen Margaret	382799	6597396	metakomatiite	–			talc; chlorite; carbonate; biotite; pyrite	Roberts et al. (in prep.)
Queen Margaret	382799	6597396	felsic volcaniclastic metasedimentary rock	–	quartz; feldspar; muscovite; chlorite; carbonate; rutile; pyrite		quartz; albite; carbonate; pyrite; rutile	Roberts et al. (in prep.)
Queenslander	331605	6622420	metagabbro–metadolerite	A	chlorite; carbonate		sericite; pyrite	Witt (1993)
Racetrack	330941	6618145	low-Mg metabasalt	A	chlorite; carbonate		sericite; carbonate; pyrite; arsenopyrite; fluorite	Witt (1993)
Railway Venture	335665	6634255	metagabbro–metadolerite; felsic volcaniclastic metasedimentary rock	A			chlorite; carbonate; plagioclase; pyrite	Witt (1993)
Red Hill	374610	6545680	metakomatiite	–	chlorite; dolomite; talc		chlorite; dolomite; pyrite	Watchorn (1998)
Redoubtable	375761	6544055	metakomatiite; porphyry	–	chlorite		biotite; pyrite; albite	Watchorn (1998)
Royal Standard	332264	6618372	low-Mg metabasalt	A	chlorite; carbonate		quartz; sericite; carbonate;	Witt (1993)
Rumbles	422553	6562704	iron-rich metasedimentary rocks	–	magnetite; cummingtonite; hornblende; actinolite; biotite; chlorite; carbonate		pyrrhotite; arsenopyrite; magnetite; cummingtonite; hornblende; actinolite; biotite; chlorite; carbonate	Newton et al. (1998)
Sand King	303921	6656147	low-Mg metabasalt	C	biotite; hornblende; calcic plagioclase; calcite; garnet; ilmenite; pyrrhotite; pyrite		quartz; biotite; calcic plagioclase; calcite; sphene; pyrrhotite; pyrite; arsenopyrite	Witt (1993)
Santa Ana	374831	6540858	low-Mg metabasalt	B	chlorite; dolomite		biotite; albite; pyrite	Watchorn (1998)
Santa Claus	424940	6565073	iron-rich metasedimentary rocks	–	magnetite; cummingtonite; hornblende; actinolite; biotite; chlorite; carbonate		pyrrhotite; arsenopyrite; magnetite; cummingtonite; hornblende; actinolite; biotite; chlorite; carbonate	Newton et al. (1998)
Santa Claus North	424819	6565514	iron-rich metasedimentary rocks	–	magnetite; cummingtonite; hornblende; actinolite; biotite; chlorite; carbonate		pyrrhotite; arsenopyrite; magnetite; cummingtonite; hornblende; actinolite; biotite; chlorite; carbonate	Newton et al. (1998)

Table A2-2 (continued)

Deposit	*MGA coordinates*		*Host rock*	*Alteration type (mafic hosts)*	*Outer alteration zone*	*Intermediate alteration zone*	*Inner alteration zone*	*Reference*
	Easting	*Northing*						
Scottish Lass	425888	6623206	high-Mg or komatiitic metabasalt	B	plagioclase; chlorite; carbonate; quartz; epidote; leucoxene; pyrrhotite; pyrite	albite; chlorite; ankerite; quartz; biotite; muscovite; leucoxene; rutile; pyrite	albite; ankerite; quartz; muscovite; leucoxene; rutile; pyrite	Roberts et al. (in prep.)
South Duke	338459	6631861	metagabbro–metadolerite	A	chlorite; carbonate		quartz; sericite; pyrite	Witt (1993)
South Gippsland Leases	380265	6644773	felsic to intermediate clastic and metavolcaniclastic rock	–			carbonate; chlorite; sericite; quartz; pyrite; chalcopyrite; rutile; tourmaline; biotite; ilmenite; galena; sphalerite	Roberts et al. (in prep.)
Surbiton	333374	6636270	low-Mg metabasalt	A	chlorite; carbonate		quartz; sericite; pyrrhotite	Witt (1993)
Three Mile Hill	327863	6577093	metagabbro–metadolerite	C	hornblende; plagioclase; biotite; quartz; garnet; calcite; pyrrhotite; ilmenite	hornblende; calcite; plagioclase; quartz; garnet; chlorite; pyrrhotite; arsenopyrite; ilmenite	ferrohornblende; calcite; plagioclase; quartz; garnet	Knight et al. (2000)
Tindals	326523	6569710	metakomatiite	–	tremolite; chlorite; talc; calcite; biotite; pyrrhotite	tremolite; chlorite; talc; calcite; biotite; pyrrhotite	tremolite; chlorite; talc; calcite; biotite	Knight et al. (2000)
Tindals	326523	6569710	metagabbro–metadolerite	C			hornblende; plagioclase; calcite; biotite; garnet; quartz	Knight et al. (2000)
Triumph	366276	6572902	metagabbro–metadolerite	?			quartz; carbonate; pyrite	Witt (1993)
Two Up	332758	6636745	high-Mg or komatiitic metabasalt	A			chlorite; carbonate; pyrrhotite	Witt (1993)
Vesuvio	333695	6634629	metagabbro–metadolerite	A			chlorite; plagioclase; leucoxene; pyrite	Witt (1993)
Vettersburg	330982	6648821	metakomatiite	–	talc; chlorite; dolomite; magnetite	talc; albite; tremolite; magnetite	amphibole; quartz; albite	Witt (1993)
Victory/Talbot	382980	6533501	metakomatiite	–	talc; dolomite; chlorite; biotite; pyrite	dolomite; muscovite; quartz; biotite; arsenopyrite	dolomite; quartz; chlorite; muscovite; pyrrhotite; pyrite	Witt (1993)
White Hope	370332	6560359	metagabbro–metadolerite	B–C?	quartz; biotite; calcite		quartz; calcic plagioclase; calcite; biotite	Witt (1993)
Whiteheads Find	376902	6658488	undifferentiated metabasalt	B			chlorite; plagioclase; carbonate; sericite; ilmenite; epidote; biotite; tourmaline; magnetite; pyrite; chalcopyrite; pyrrhotite	Roberts et al. (in prep.)
Wombola (Just-in-Time)	389873	6572035	metagabbro–metadolerite	B	chlorite; carbonate		carbonate; sericite; plagioclase; pyrite; biotite	Roberts et al. (in prep.)
Woolshed	330297	6619541	low-Mg metabasalt	A			chlorite; quartz; pyrite	Witt (1993)
Wycheproof	336476	6644800	low-Mg metabasalt and porphyry	B	biotite; chlorite; calcite; sphene; epidote; pyrrhotite; pyrite		quartz; ankerite; albite; muscovite; rutile; pyrite	Witt (1993)
Zoroastrian	335302	6642841	metagabbro–metadolerite	A			carbonate; chlorite; sericite; pyrrhotite	Witt (1993); Bottomer and Robinson (1990)

References

BARTSCH, R. D., 1990, Lady Bountiful gold deposit, *in* Geology of the mineral deposits of Australia and Papua New Guinea, Volume 1 *edited by* F. E. HUGHES: Australasian Institute of Mining and Metallurgy, Monograph 14, p. 401–404.

BECKETT, T. S., FAHEY, G. J., SAGE, P. W., and WILSON, G. M., 1998, Kanowna Belle gold deposit, *in* Geology of Australian and Papua New Guinean mineral deposits *edited by* D. A. BERKMAN and D. H. MACKENZIE: Australasian Institute of Mining and Metallurgy, Monograph 22, p. 201–206.

BOTTOMER, L. R., and ROBINSON, C., 1990, Bardoc gold deposits, *in* Geology of the mineral deposits of Australia and Papua New Guinea, Volume 1 *edited by* F. E. HUGHES: Australasian Institute of Mining and Metallurgy, Monograph 14, p. 385–388.

CLOUT, J. M. F., CLEGHORN, J. H., and EATON, P. C., 1990, Geology of the Kalgoorlie gold field, *in* Geology of the mineral deposits of Australia and Papua New Guinea, Volume 1 *edited by* F. E. HUGHES: Australasian Institute of Mining and Metallurgy, Monograph 14, p. 411–431.

COPELAND, I. K., and THE GEOLOGICAL STAFF OF NEW HAMPTON GOLDFIELDS NL, 1998, Jubilee gold deposit, Kambalda, *in* Geology of Australian and Papua New Guinean mineral deposits *edited by* D. A. BERKMAN and D. H. MACKENZIE: Australasian Institute of Mining and Metallurgy, Monograph 22, p. 219–224.

GEBRE-MARIAM, M., 1994, The nature and genesis of Archaean mesozonal to epizonal gold deposits of the Mt Pleasant area, near Kalgoorlie, Western Australia: University of Western Australia, PhD thesis (unpublished).

GLASSON, M. J., HENDERSON, R. G., and TIN, M., 1998, Broads Dam gold deposits, *in* Geology of Australian and Papua New Guinean mineral deposits *edited by* D. A. BERKMAN and D. H. MACKENZIE: Australasian Institute of Mining and Metallurgy, Monograph 22, p. 197–200.

HANCOCK, M. C., ROBERTSON, I. G., and BOOTH, G. W., 1990, Paddington gold deposits, *in* Geology of the mineral deposits of Australia and Papua New Guinea, Volume 1 *edited by* F. E. HUGHES: Australasian Institute of Mining and Metallurgy, Monograph 14, p. 395–400.

HARRISON, N., BAILEY, A., SHAW, J. D., PETERSEN, G. N., and ALLEN, C. A., 1990, Ora Banda gold deposits, *in* Geology of the mineral deposits of Australia and Papua New Guinea, Volume 1 *edited by* F. E. HUGHES: Australasian Institute of Mining and Metallurgy, Monograph 14, p. 389–394.

IVEY, M. E., FOWLER, M. J., GENT, P. G., and BARKER, A. J., 1998, Centurion gold deposits, Binduli, *in* Geology of Australian and Papua New Guinean mineral deposits *edited by* D. A. BERKMAN and D. H. MACKENZIE: Australasian Institute of Mining and Metallurgy, Monograph 22, p. 215–218.

KNIGHT, J. T., RIDLEY, J. R., and GROVES, D. I., 2000, The Archaean amphibolite facies Coolgardie goldfields, Yilgarn Craton, Western Australia: nature, controls, and gold field-scale patterns of hydrothermal wall-rock alteration: Economic Geology, v. 95, p. 49–84.

NEWTON, P. G. N., SMITH, B., BOLGER, C., and HOLMES, R., 1998, Randalls gold deposits, *in* Geology of Australian and Papua New Guinean mineral deposits *edited by* D. A. BERKMAN and D. H. MACKENZIE: Australasian Institute of Mining and Metallurgy, Monograph 22, p. 219–224.

PYKE, D., 1990, Gibraltar gold deposit, *in* Geology of the mineral deposits of Australia and Papua New Guinea, Volume 1 *edited by* F. E. HUGHES: Australasian Institute of Mining and Metallurgy, Monograph 14, p. 475–477.

RANSTED, T. W., 1990, Eureka gold deposit, *in* Geology of the mineral deposits of Australia and Papua New Guinea, Volume 1 *edited by* F. E. HUGHES: Australasian Institute of Mining and Metallurgy, Monograph 14, p. 383–384.

ROBERTS, F. I., WITT, W. K., and WESTAWAY, J., in prep., Gold mineralization in the Edjudina–Kanowna region, Eastern Goldfields, Western Australia: Western Australia Geological Survey, Report 90.

SCHILLER, J. C., and IVEY, M. E., 1990, Hannans south gold deposit, *in* Geology of the mineral deposits of Australia and Papua New Guinea, Volume 1 *edited by* F. E. HUGHES: Australasian Institute of Mining and Metallurgy, Monograph 14, p. 443–447.

TAYLOR, T., 1984, The palaeoenvironment and volcanic setting of Archaean volcanogenic rocks in Kanowna district, near Kalgoorlie, Western Australia: University of Western Australia, MSc thesis (unpublished).

WATCHORN, R. B., 1998, Kambalda–St Ives gold deposits, *in* Geology of Australian and Papua New Guinean mineral deposits *edited by* D. A. BERKMAN and D. H. MACKENZIE: Australasian Institute of Mining and Metallurgy, Monograph 22, p. 243–254.

WITT, W. K., 1993, Gold mineralization in the Menzies–Kambalda region, Eastern Goldfields, Western Australia: Western Australia Geological Survey, Report 39, 165p.

WITT, W. K., 1994, Geology of the Melita 1:100 000 sheet: Western Australia Geological Survey, 1:100 000 Geological Series Explanatory Notes, 63p.

MIKUCKI AND ROBERTS

Metamorphic petrography of the Kalgoorlie Region
Eastern Goldfields Granite-Greenstone Terrane: METPET database

RECORD 2003/12

Further details of geological publications and maps produced by the Geological Survey of Western Australia can be obtained by contacting:

Information Centre
Department of Industry and Resources
100 Plain Street
East Perth WA 6004
Phone: (08) 9222 3459 Fax: (08) 9222 3444
www.doir.wa.gov.au